Compression and Time-Dependent Behaviour in Danish Clays and Chalk - An Experimental Study

Peri, Elena

DOI (link to publication from Publisher):
10.5278/vbn.phd.tech.00054

Publication date:
2021

Document Version
Publisher's PDF, also known as Version of record

COMPRESSION AND TIME-DEPENDENT BEHAVIOUR IN DANISH CLAYS AND CHALK – AN EXPERIMENTAL STUDY

BY
ELENA PERI

DISSERTATION SUBMITTED 2021

AALBORG UNIVERSITY
DENMARK

COMPRESSION AND TIME-DEPENDENT BEHAVIOUR IN DANISH CLAYS AND CHALK - AN EXPERIMENTAL STUDY

PhD thesis

Elena Peri

AALBORG UNIVERSITY
DENMARK

Thesis submitted 6th February, 2021

Dissertation submitted: February 2021

PhD supervisor: Prof. Lars Damkilde
Aalborg University

PhD committee: Professor John Dalsgaard Sørensen (Chairman)
Aalborg University

GEO Engineering Director, Ph.D. Lindita Kellezi
GEO

Professor, Dr.-Ing. Martin Achmus
University of Hannover

PhD Series: Faculty of Engineering and Science, Aalborg University

Department: Department of the Build Environment

ISSN (online): 2446-1636
ISBN (online): 978-87-7210-893-3

Published by:
Aalborg University Press
Kroghstræde 3
DK – 9220 Aalborg Ø
Phone: +45 99407140
aauf@forlag.aau.dk
forlag.aau.dk

Printed in Denmark by Rosendahls, 2021

PREFACE

This thesis “Compression and time-dependent behaviour in Danish clays and chalk - an experimental study” is the result of a Ph.D. study carried out from January 2018 to January 2021 at the Department of the Built Environment, Aalborg University, Denmark. The thesis has been submitted for assessment in partial fulfilment of the Ph.D. degree. As part of the assessment, co-author statements have been made available to the assessment committee.

This thesis is based on five scientific publications. Three of them are scientific papers submitted to different journals (Papers A, B and E). Two are conference papers: Papers C presented at the 7th International Symposium on Deformation Characteristics of Geomaterials, Glasgow 2019, and Paper D presented at the Nordic Geotechnical Meeting, virtual event held in 2021. The Ph.D. included a collaboration with Deltares in Delft, The Netherlands. The joint study produced Paper A.

Acknowledgments

I would like to acknowledge the advice received from my supervisor Professor Lars Damkilde, his guidance helped me during my studies. I thank Professor Cor Zwanenburg from Deltares, for the discussions and comments that enriched my research. My special gratitude goes to Dr. Aleksandra Koteras, my office mate with whom I have shared more than research discussions.

CV

Elena Peri

elena.peri91@gmail.com

Professional experience

January 2018-January 2021	Ph.D. Researcher in geotechnical engineering at the Built Department at Aalborg University, Denmark.
June 2017 – January 2018	Project Geotechnical Engineer at Enser Engineering, Bologna, Italy.
January 2017-April 2017	Internship at Deltares, Delft, The Netherlands.

Education

2016	Master thesis "An investigation on the behavior of a shallow foundation resting on a layered soil near a slope". UWA, University of Western Australia, Perth, Australia.
2010-2016	Combined Bachelor and Master in Building Engineering, School of Engineering and Architecture, Bologna University.

Courses at a Ph.D. level

- Advanced Soil Modeling, Trondheim University, Norway.
- Introduction to Python coding language.
- Management of research and development.
- Quantitative risk assessment in geotechnical engineering.
- Design and analysis of experiments with R.
- Writing and reviewing of scientific papers.
- Bayesian statistics, simulation and software – with a view to application examples.
- Academic information searching, publishing and management.

Publications

Conference papers

- Peri Elena, Nielsen S. D., Nielsen B.N. and Ibsen, L. B., 2019, *Consequences of slenderness and boundary conditions in triaxial testing on the reliability of design parameters.* 7th International Symposium on Geotechnical Safety and Risk (ISGSR 2019): State-of-the-Practice in Geotechnical Safety and Risk. Research Publishing.

- Nielsen Søren Dam, Peri E. and Nielsen B.N., 2019, *Evaluation of Preparation Techniques of Chalk Samples for Oedometer Testing.* 17th European Conference on Soil Mechanics and Geotechnical Engineering - Reykjavík, Iceland: Geotechnical Engineering foundation of the future. The Icelandic Geotechnical Society.

- Peri Elena, Nielsen S.D., Nielsen B.N. and Ibsen L.B., 2019, *New interpretation for consolidation modulus on chalk.* 17th European Conference on Soil Mechanics and Geotechnical Engineering - Reykjavík, Iceland: Geotechnical Engineering foundation of the future. The Icelandic Geotechnical Society.

- Peri Elena, Ibsen L.B. and Nielsen B.N., 2019, *How to interpret consolidation and creep in Yoldia clay.* 7th International Symposium on Deformation Characteristics of Geomaterials, IS-Glasgow 2019. Tarantino, A. & Ibraim, E. (ed.). EDP Sciences, (E3S Web of Conferences, Bind 92).

- Peri Elena, Ibsen L.B. and Nielsen B.N., 2019, *Influence of sample slenderness and boundary conditions in triaxial test – a review.* 7th International Symposium on Deformation Characteristics of Geomaterials, IS-Glasgow 2019. Ibraim, E. & Tarantino, A. (ed.). EDP Sciences, (E3S Web of Conferences, Bind 92).

- Peri Elena, Nielsen S.D., Nielsen B.N. and Damkilde L., 2021, *Experimental evaluation of time effect on swelling pressure in high plasticity clay.* Proceedings of the Nordic Geotechnical Meeting 2020 (In press).

Journal papers

- Peri Elena, Zwanenburg C., Damkilde L., *Determination of preconsolidation pressure by different methods of interpretation*. Submitted to Engineering Geology, 2020.

- Peri Elena, Nielsen S.D. and Nielsen B.N., *Geotechnical recommendation for preparation, execution and interpretation of oedometer test on chalk*. Submitted to Geotechnical and Geological Engineering, 2020.

- Peri Elena, Koteras A., Damkilde L., *Modelling the compressive behaviour of soft soil by validating laboratory results*. Submitted to Geomechanics and Engineering, 2020.

Report

- Nielsen Søren Dam, Peri E. and Nielsen B.N., 2018, *Data report on Rørdal Chalk.* Aalborg: Aalborg Universitet, Institut for Byggeri og Anlæg. 20 s. (DCE Technical reports; Nr. 257).

SUMMARY

The compressive behaviour and settlements of a soil deposit affect the performance of an over structure during all its life, from the ground improvement work before the construction, until the long-term period. To guarantee an optimal geotechnical design of the construction, it is important to investigate different aspects of soil compression behaviour, for example, the swelling potential of the underneath soil after an excavation before construction or the creep behaviour in the long-term. Therefore, it is fundamental to carry out a high quality-testing program, which usually requires a high cost and a long time. For this reason, the quality of testing is too often neglected, and this leads to an approximated interpretation of soil parameters.

This thesis investigates the compression behaviour of a set of Danish clays and chalk, in relation to laboratory procedure, interpretation of results and influence of testing time. The experimental program comprises oedometer tests and constant volume swelling tests. The investigation covers, among others, Rørdal chalk, chalk found at variable depth in North Denmark and similar to the North Sea reservoir chalk, and Søvind Marl, a fissured clay with extremely high plasticity and swelling potential. Other oedometer tests were run on Aalborg clay, a clay characterised by thin sand layers. A database containing oedometer results on medium-stiff clays contributed to the investigations about the preconsolidation stress interpretation and the numerical validation through different constitutive soil models.

The results obtained from testing Rørdal chalk and Søvind Marl clarify the influence of testing time on the interpretation of soil parameters. The long-lasting tests on chalk define the optimal procedure and equipment to deal with this material. Running swelling tests on Søvind Marl demonstrates that the full swelling potential could take weeks to develop. The preconsolidation pressure analysis on various Danish clays shows the variability of this parameter and the effect of the testing methodology on the results. In the final part of the project, different constitutive soil models represent the compressive behaviour of soft soil. The validation of oedometer tests proves how different soil models can simulate oedometer tests on Danish medium-stiff clays. The precautions presented in the papers, concerning both the laboratory procedure and the interpretation of the results, if introduced in the engineering practice, could improve the stiffness properties and settlement prediction useful to the geotechnical design.

This thesis is a collection of five papers. Paper A deals with the interpretation of preconsolidation stress for different medium-stiff clays from Denmark. Paper B contributes with a guideline for the interpretation of oedometer tests on Rørdal chalk. Paper C interprets consolidation and creep strains and preconsolidation stress in Yoldia and Aalborg clays. Paper D shows the results of long-lasting constant volume swelling tests on Søvind Marl. Paper E presents some numerical validations of oedometer tests on medium stiff clays through different soil models.

RESUME

En jords sammentrykkelighed og sætningsfølsomheden påvirker ydeevnen af en overkonstruktion i hele dens levetid, fra jordforbedringsarbejdet før konstruktionen indtil den langvarige periode. For at garantere et optimalt geoteknisk design af konstruktionen er det vigtigt at undersøge forskellige aspekter af jords sammentrykkelighed, for eksempel hævelsespotentialet for den underlæggende jord efter en udgravning før konstruktion eller krybeopførsel på lang sigt. Derfor er det grundlæggende at gennemføre et testprogram af høj kvalitet, som normalt kræver høje omkostninger og lang tid. På grund af dette er testkvaliteten ofte negligeret, hvilket fører til en ringere forståelse af jordparametre.

Denne afhandling undersøger hvordan forskellige dansk ler og kridt opfører sig under sammentrykning i forhold til laboratorieprocedurer, tolkning af resultater og indflydelsen af tid under testen. Det eksperimentelle program omfatter konsolideringsforsøg og svelletest med konstant volumen. Undersøgelsen dækker blandt andet Rørdal-kridt som findes på variabel dybde i Norddanmark og den svarer til Nordsøens reservoirkridt, og Søvind Marl som er en sprækket lertype med ekstremt høj plasticitet og hævelsespotentiale. Andre konsolideringsforsøg blev udført på Aalborg ler som er karakteriseret ved tynde sandlag. En database, som indeholder resultater af konsolideringsforsøg på mellemstive lertyper, bidrog til undersøgelserne om fortolkning af forbelastningstrykket og den numeriske validering ved hjælp af forskellige konstituerende jordmodeller.

Resultaterne opnået ved testning af Rørdal-kridt og Søvind Marl tydeliggør testtidens indflydelse på fortolkningen af jordparametre. De langvarige forsøg på kridt definerer den optimale procedure og udstyr til at håndtere dette materiale. Udførelse af svelle-forsøg på Søvind Marl viser, at det kan tage uger at udvikle det fulde hævelsespotentiale. Forbelastningstrykketanalysen på forskellige danske lertyper viser variabiliteten af denne parameter og effekten af testmetoden på resultaterne. I den sidste del af afhandlingen anvendes forskellige konstitutive jordmodeller til at repræsentere den komprimerende egenskab af blød jord til den numeriske validering. Valideringen beviser, hvordan forskellige jordmodeller kan simulere konsolideringsforsøg af de danske mellemstive lertyper. Artiklerne introducerer forholdsregler vedrørende både laboratorieproceduren og tolkning af resultaterne. Hvis disse forholdsregler blev inkluderet i ingeniørpraksis kunne de forbedre estimeringen af stivhedsegenskaberne og sætningsegenskaberne af jordens, hvilket er nyttig information til det geotekniske design.

Denne afhandling ineholder 5 artikler. Artikel A beskriver tolkning af forbelastningstrykket for forskellige mellemstive lertyper fra Denmark. Artikel B bidrager med en retningslinje til tolkning af konsolideringsforsøg på Rørdal kridt. Artikel C fortolker konsolidering og krybe-tøjninger og forbelastningstrykket i Yoldia

og Aalborg ler. Artikel D viser resultaterne af langvarige svelletest med konstant volumen på Søvind Marl. Artikel E præsenterer nogle numeriske valideringer af konsolideringsforøger på mellemstive lertyper gennem forskellige jordmodeller.

TABLE OF FIGURES

TABLE OF CONTENTS

CHAPTER 1. INTRODUCTION

1.1. BACKGROUND

Soil is a three-phase material, composed of mineral particles, water and air. Unlike rocks, soils are a relatively weak material, and applied stresses can lead to significant deformations. Soil deformations depend on soil initial state, stress history, stress path and time.

When a load is applied to a saturated soil deposit, the water is squeezed out of the pores. A volume change occurs, and the soil stratum settles down. This process is known as consolidation. When the consolidation is over, i.e., the excess pore water pressure has dissipated, the soil deposit exhibits time-dependent deformations under constant load, the creep deformations, that are due to deformation in the soil skeleton. Some soils do not exhibit only a reduction in volume when consolidate, but also show a volume expansion when the water content increases. In some cases, a heave appears on the soil surface.

It is fundamental to predict the soil deformations underneath a structure to not compromise the serviceability of it. A safe design implies that the deformations of a soil deposit under the infrastructure or structure do not cause any damage. A practical example of soil consolidation is a ground improvement intervention with preloading using an embankment (see Fig. 1). Such a process fastens the consolidation of a soil deposit before the construction work and makes the soil deposit a more appropriate foundation. To design an adequate embankment, the prediction of the deposit settlements over time needs careful investigation, as well as the development of excess pore pressure.

It is well known that foundations laying on clayey layers are subjected to settlements for a long period, continuing at a steadily decreasing rate, but still appreciable after several years. When a soil deposit is investigated, before it is going to support any kind of construction, two important matters need an answer. The first one is to estimate what will be the final settlement of the structure. Secondly, the time that it will take to develop this settlement. Oedometer testing is a laboratory test that investigates deformation parameters useful to answer these questions.

1.2. CONSOLIDATION THEORY

Karl Terzaghi started in the 1920s to develop the first contribution to the consolidation theory. Terzaghi intended to evaluate the relationship between time and settlement and designed the oedometer, which worked as a support for his one-dimensional consolidation theory. In Terzaghi (1943), he stated that "*Every process involving a decrease of water content of a saturated soil without replacement of the water by air is called a process of consolidation*". When a saturated clay deposit is loaded, the load

increase is initially taken by the water and generates an excess pore pressure. With time, the water escapes the soil pores, and the load increment is transferred to the soil particles. This causes the soil layer to settle. In other words, during the consolidation process, the excess pore pressure dissipates, and the soil particles are packed more tightly, meaning that the soil deposit settles. While the pore pressure decreases, the effective stress increases (see Fig. 2).

The one-dimensional consolidation theory by Terzaghi describes the spatial-temporal variation of excess pore pressure through the primary consolidation coefficient. The coefficient of consolidation c_v in equation (1.1) is the rate at which the soil undergoes the consolidation. Terzaghi's theory of consolidation and its non-dimensional time factor T_v relate c_v to a certain time t, needed to reach a specific degree of consolidation, and H_{dr}, drainage path of water. The root time method described by Taylor (1948) estimates c_v = 0.848 at a time equal to T_{90}, the time necessary to complete the 90% consolidation, equation (1.2).

$$\frac{\partial u}{\partial t} = c_v \frac{\partial u^2}{\partial z^2} \tag{1.1}$$

$$c_v = \frac{T_{90} \cdot H_{dr}^2}{t_{90}} \tag{1.2}$$

Taylor continued the research about the consolidation and introduced the importance of the plastic time lag, a phenomenon not considered in Terzaghi's theory (Taylor, 1948). Terzaghi neglected the existence of secondary compression at the end of primary consolidation when the excess pore pressure is dissipated, and the load is constant. Instead, Taylor identified three parts of the total compression during a single oedometer loading increment: 1) the initial/immediate compression, 2) the primary compression, and 3) the secondary compression or creep. The sample is compressed at high speed at the beginning of the consolidation, while the speed of compression steadily decreases during the secondary compression.

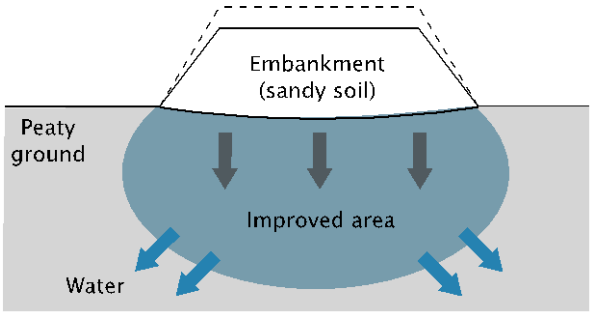

Fig. 1. Consolidation due to preloading in ground improvement intervention.

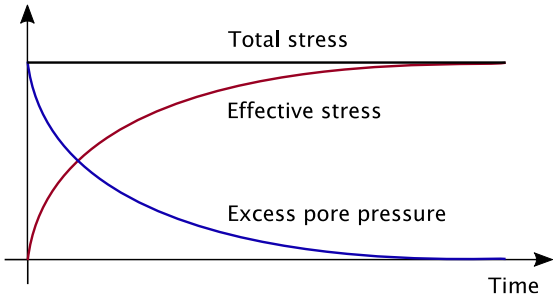

Fig. 2. Pore pressure and stress variation during the consolidation process.

1.3. OEDOMETER TESTING: PRELIMINARIES

The oedometer test is a fundamental procedure, widely used in geotechnical laboratories. The soil sample is horizontally confined in a ring, and a load vertically applied to it. This procedure investigates the one-dimensional consolidation of the soil sample and returns its deformation properties. An incremental load oedometer test (ILO) involves consecutive steps where increasing loads are applied to the sample. When a clay sample is subject to a constant load, its void ratio decreases with time. Fig. 3 shows the typical output of a single load step in a log*(t)*-*e* graph. The first part of the curve is related to the primary consolidation, controlled by the dissipation of pore excess water. The second part of the curve is creep deformation, defined by the secondary compression index C_α. It is common practice to let each load increment acting for 24 hours, but the full primary consolidation can be completed in shorter or longer times.

The sequence of applied stress typically consists of doubling each subsequent stress ($\Delta\sigma'/\sigma' = 1$). This practice, also suggested by the ISO 17892-5: 2017, guarantees a sequence of evenly spaced points. When the oedometer test is completed, the sequence of deformations from each load step returns the compression curve represented in the semilogarithmic plane log*(σ')*-*e* (see Fig. 4). This curve generally shows a bilinear behaviour. The first part of the consolidation curve, the recompression line, presents smaller and elastic deformations; instead, in the second part, the soil exhibits a softer response and plastic deformations. From the recompression line, it is possible to determine the recompression index C_r, and, from the virgin compression line, the compression index C_c.

Fine-grained soil exhibits 'memory' of the stress history previously experienced. The soil structure saves information about earlier stress states. In the zone where the compression curve shows a knee, the preconsolidation stress σ'_p finds place. This value is defined as the highest effective stress that the soil was ever subjected to.

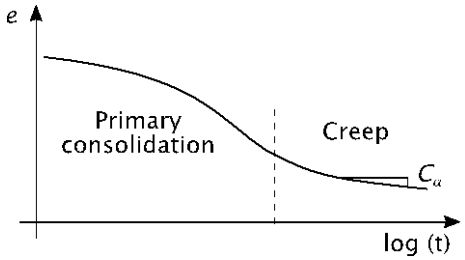

Fig. 3. Example of the time-deformation curve of a single load step.

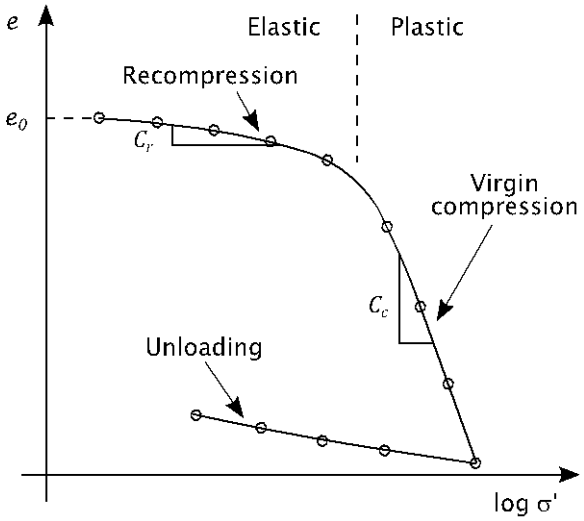

Fig. 4. Final compression curve returned by the oedometer test.

CHAPTER 2. AIM OF THE THESIS AND RESEARCH PROJECT

2.1. MOTIVATION AND GENERAL SCOPE

The soil deformation properties resulting from oedometer testing, like stiffness and creep parameters, are fundamental input for the definition of soil models. Only careful laboratory investigation and interpretation lead to a realistic understanding of the deformation properties and the soil behaviour. However, the oedometer test remained a procedure generally unchanged since it was introduced, and it is common practice to conduct oedometer testing by minimizing the testing time and treating different soils with the same procedure.

This Ph.D. project aims to a better understanding of the specific compressive behaviour of different kinds of Danish soils, and its objective is to find the most accurate laboratory methodology and interpretation for each of them. An oedometer testing program was carried out to investigate the deformation properties and stress history of the soils. Part of the study focuses on finding the most accurate and consistent method to interpret the stress history of a set of Danish clays. An experimental program on Rørdal chalk evaluates the relationship between testing time and long-term chalk behaviour. Swelling tests on Søvind Marl predict the long-term swelling potential of this clay. The testing programs give special attention to the testing time and influence of the laboratory methodology on the resulting deformation properties.

2.2. SPECIFIC OBJECTIVES

1. Influence of separation of strain on the interpretation of preconsolidation pressure.
2. Interpretation of preconsolidation pressure for different Danish clays.
3. Understanding of compressive behaviour of Rørdal chalk.
4. Interpretation of constant volume swelling of Søvind Marl.
5. Understanding the performance of different constitutive soil models by numerically validating ILO tests.

2.3. RESEARCH PROJECT

To achieve the specific aims listed above, the following process was followed.

1. ILO tests were performed on Yoldia clay, with a focus on the separation of strains methods and preconsolidation pressure interpretation.
2. After the ILO on Yoldia clay, some questions on the interpretation of preconsolidation stress were raised. Therefore, different interpretation methods

of preconsolidation stress were compared for different clays. Moreover some ILO validation tests on remoulded clay were performed with pre-applied stress.

3. Performing ILO on Rørdal chalk, with load steps lasting 14 days.
4. Performing constant volume swelling test on Søvind Marl and comparison between different swelling duration. ILO test followed the swelling tests.
5. Validation of ILO in Plaxis by using different soil models (Hardening Soil, Soft Soil Creep and Creep-SCLAY1S models).

Fig. 5 illustrates a graphical overview of the research and a summary of the papers attached in the appendix.

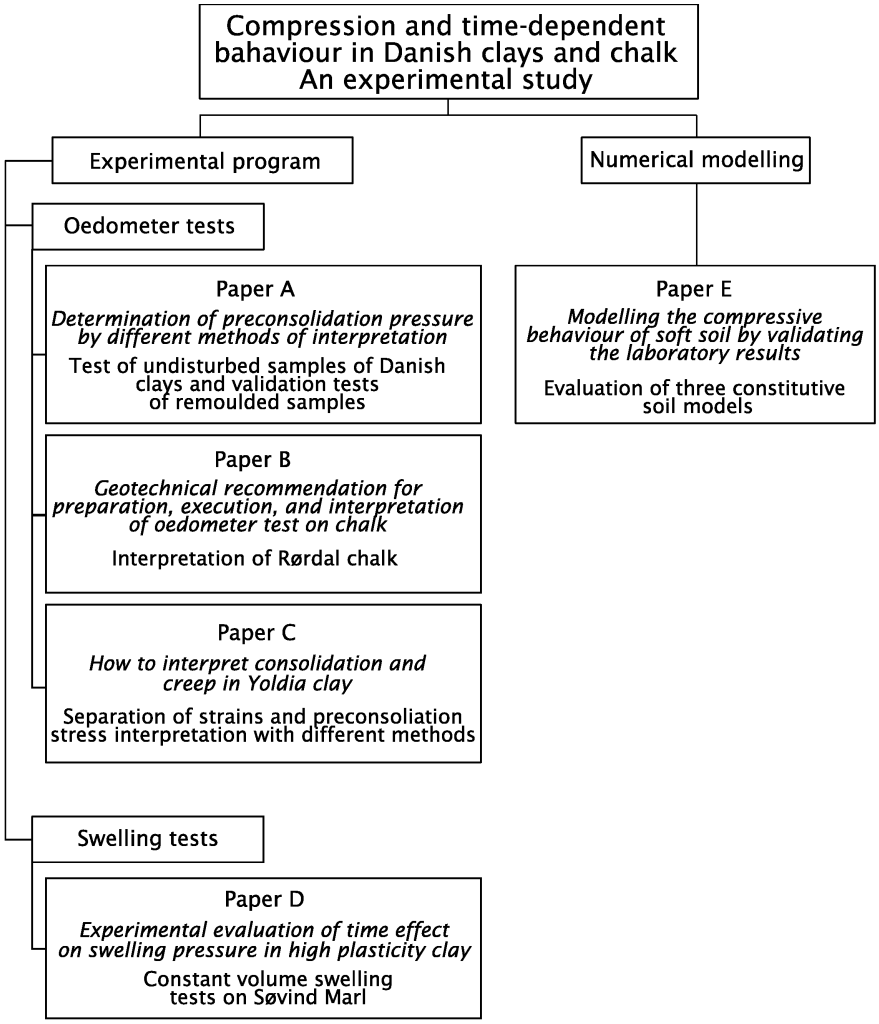

Fig. 5. Overview of the research project and papers.

CHAPTER 3. GENERAL DESCRIPTION OF THE SOILS

This thesis presents the results of ILO and swelling tests for different soils. Paper A shows the interpretation of preconsolidation stress for clays from various locations in Denmark. These clays differ in depth, age and compressibility properties. Paper B investigates the deformation properties of Rørdal chalk from Aalborg. Paper C presents the results of tests on Aalborg Clay and Yoldia Clay. Paper D investigates the effect of time on the development of swelling pressure for Søvind Marl, a high plasticity Eocene clay. Rørdal chalk and Søvind Marl have some unique characteristics, and a more in-depth analysis is presented hereafter.

Many geological events shaped the geology of Denmark over millions of years; however, what is visible today is the result only of the most recent glacial and postglacial ages during the Quaternary period. Under this most recent layer, older formations are dating back to more than one billion years. For example, in Northern Jutland and Eastern Zealand, the pre-Quaternary layer is formed of late cretaceous and Dania chalk; instead, plastic Paleogene clay is found in eastern Jutland and Funen (Nielsen, 1995). Fig. 6 divides in colour bands the pre-Quaternary geology of Denmark.

3.1. RØRDAL CHALK

In the North Sea basin, chalk is present both onshore and offshore. In offshore oil reservoirs, such as the Ekofisk oil field, the presence of chalk can lead to problems of subsidence beneath the extraction platforms (Alam et al., 2012; Dahou et al., 1995; Delage et al., 1996; Homand and Shao, 2000; Maranini and Brignoli, 1999).

North Sea chalk is mainly composed of the debris of coccoliths, calcium carbonate plates formed by algae, of size equal to about 10 μm (Fabricius, 2007; Risnes and Flaageng, 1999; Stenestad, 2006). Samples from different locations vary in many properties, for example, for the presence of microfossils and coccoliths, level of calcite cementation, porosity, carbonate content, gas permeability (Hjuler and Fabricius, 2009). In the literature, chalk is treated differently: some research considers it a fine-grained sedimentary rock (Hjuler and Fabricius, 2009; Korsnes et al., 2008), others handle it like soil (Leth et al., 2016) or describe it as a material between a poroelastic rock and a disaggregated material with yield zone and soil mechanical characteristics (Kågeson-Loe et al., 1993).

Considering this variability, it is important to test specifically the chalk of interest, instead of relying only on previous and generic studies. This thesis discusses the compressive behaviour of Rørdal chalk. This kind of chalk formed during the

Maastrichtian Age, the period that spanned from 72.1 to 66 million years ago, and it presents high porosity. The analysed samples originate from the Rørdal quarry, located in eastern Aalborg. In this area, the chalk is present from the surface level to a variable depth between 500-750 m (Japsen, 2000). Other researchers that investigated Rørdal chalk are Håkansson et al. (1974), Leth et al. (2016), Stenestad (2006) and Strand et al. (2007). Some pictures captured by a stereomicroscope show 3D details of the chalk surface (Fig. 7).

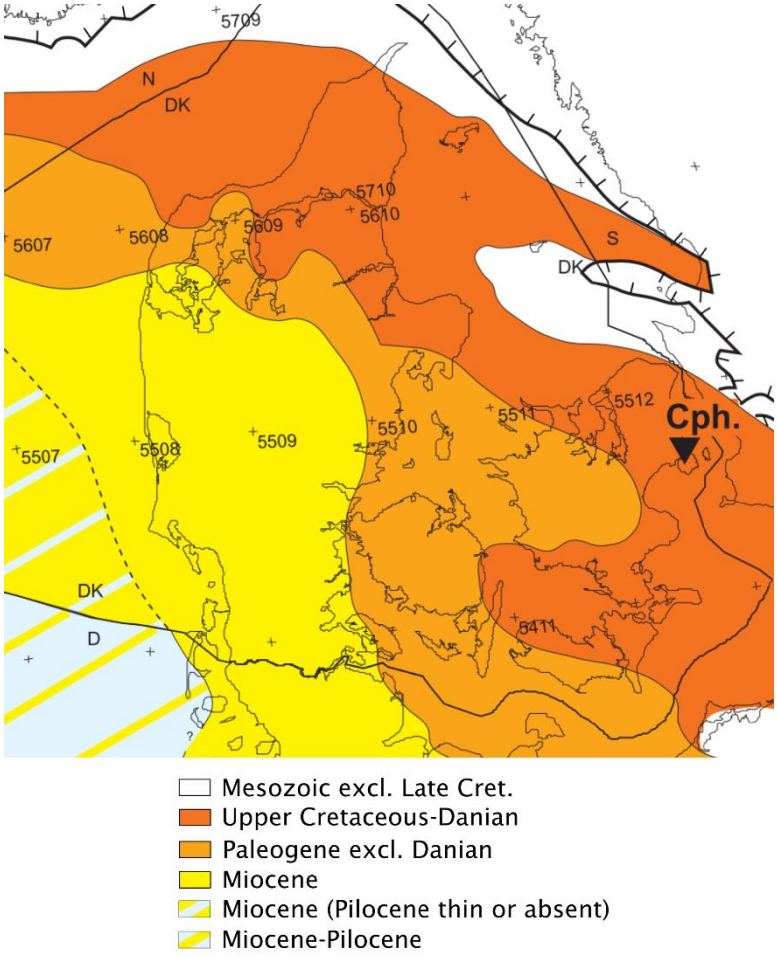

Fig. 6. The pre-Quaternary geology of Denmark adapted from Japsen (1998).

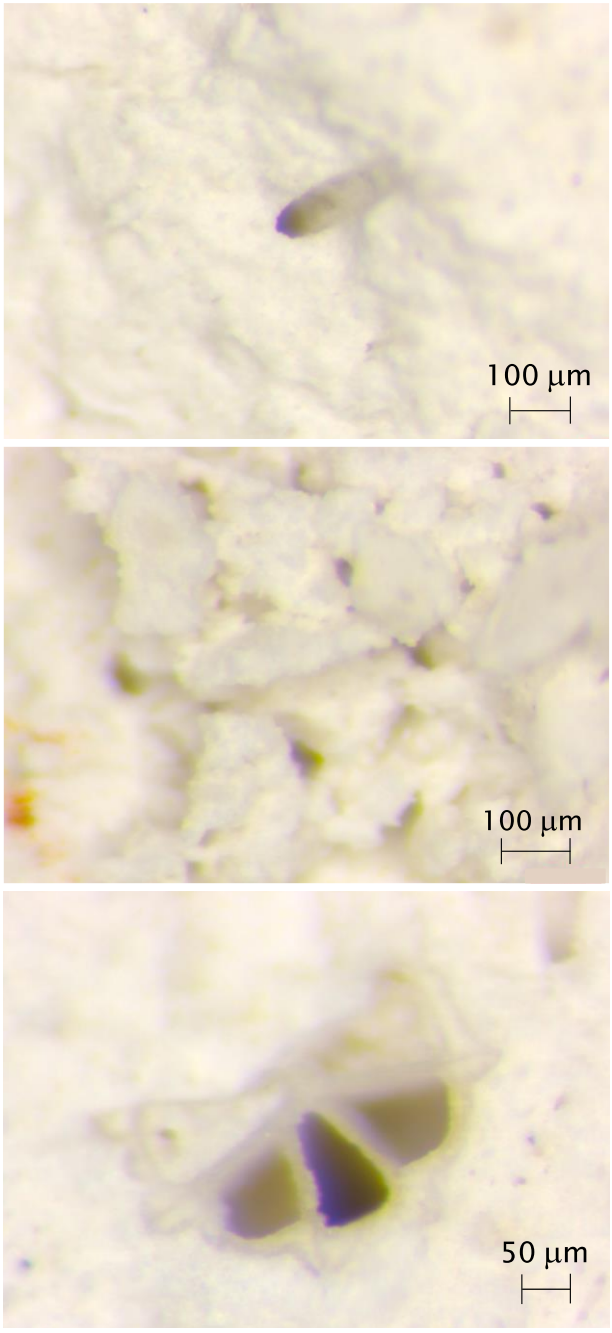

Fig. 7. Images of Rørdal chalk core samples taken by stereomicroscope.

3.2. SØVIND MARL

At the beginning of the Eocene era, which started 56 million years ago, Denmark was partly covered by water. The volcanic activity between Greenland and North-western Europe increased after the transition between the Paleocene and Eocene eras. The water level raised again after the beginning of the Eocene era, and, in the North Sea, all sediments following this period are very fine-grained plastic clays, originating from the chemical weathering of volcanic materials. Layers up to 200 m of plastic clay were deposited during the middle and late Eocene era (Heilmann-Clausen, 2010). These clays belong to three formations: Røsnes Clay, Little Belt Clay and Søvind Marl, from the oldest to the youngest, respectively (Heilmann-Clausen et al., 1985). From the Oligocene age, younger deposits covered and loaded the Søvind Marl. Further ice ages in the Quaternary period contributed to load and unload the Søvind Marl (Heilmann-Clausen, 2010). The unloading made the clay swelling, and this resulted in a large number of fissures running through the soil layer.

These events made the Søvind Marl a highly overconsolidated clay, characterized by a special difficulty in identifying its preconsolidation stress. Krogsbøll et al. (2012) suggested that the debonding during laboratory tests causes the Danish Paleogene clays to ‘forget’ the preconsolidation stress, and so, to ‘lose their memory’. The Søvind Marl compression curves show a progressive and smooth yielding, instead of the typical bilinear behaviour. Previous studies identify two yield stresses in the compression curve of Søvind Marl, where the second-highest stress is the one related to geological preloading (Grønbech et al., 2015a; Okkels and Hansen, 2016).

The Søvind Marl is also characterized by high plasticity and high swelling potential. Smectite is the clay mineral with the highest concentration (between 35-45%), and it is the cause of high plasticity and tendency to expand. The calcite content affects the colour of the clay, which varies from dark grey to whiter as the calcite increases (Grønbech et al., 2015a).

The Søvind Marl samples tested in this thesis originate from Aarhus Harbour. At this location, the Søvind Marl layer was found starting from a depth equal to 11-12 m (Grønbech et al., 2015b), and the tested samples come from 35 and 63 m depth. Fig. 8 shows one of the samples during the preparation for the swelling test.

Fig. 8. Sample preparation of Søvind Marl in the oedometer ring.

3.3. DANISH CLAYS

Paper C deals with clays from Nørre Lyngby and Aalborg, Paper A and Paper E present some additional ILO results of different Danish clays from an existing data set. These clays come from various locations and present different characteristics for aspect, depth, and period of origin.

During the last glacial period, the Weichselian, Northern Europe and Scandinavia were covered by ice. When the ice sheet began to melt between 18,000 and 13,000 years BP (Lagerlund and Houmark-Nielsen, 1993), the water covered a depressed area, including the north part of Denmark, forming the Yoldia Sea where marine sediments deposited. Samples of Nørre Lyngby clay contain Yoldia mussels and, therefore, are called Yoldia clay. The most superficial clay in this area was dated about 14,650-12,650 years BP (Lagerlund and Houmark-Nielsen, 1993; Richardt, 1996). Abrahamsen and Readman (1980) define the clay Younger Yoldia clay, which varies between argillaceous sand and fine-grained clay.

The Aalborg clay also belongs to the late glacial period. This clay does not contain mussels, and it is characterized by the presence of sand due to the summer-winter alternation (Iversen et al., 2010), see Fig. 9. On the other hand, a clay containing

molluscan fossils is the Gram clay from Rømø, belonging to the late Miocene and described by Piasecki (1980). Other samples from Anholt belong to the Eemian interglacial period (late Pleistocene) and were taken from about 77 meters depth. The most recent samples present in this research are the two samples from Skagen. They belong to the Holocene period and are sandy silty marine clay. Their depth of origin is equal to about 35-40 m below the sea level.

Fig. 10 shows the sample's area of origin and summarizes some of their peculiar features.

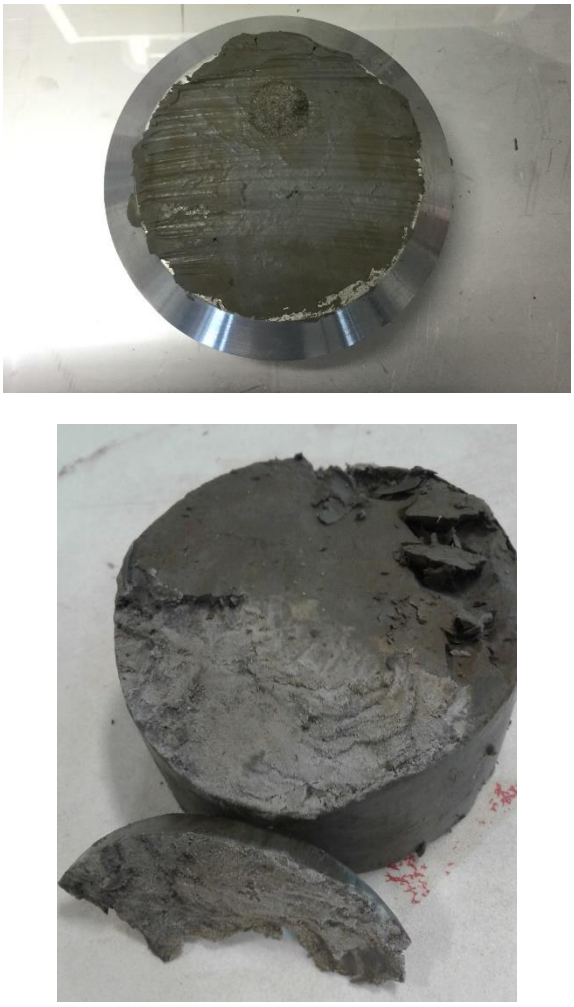

Fig. 9. Samples of Aalborg clay with sand layers.

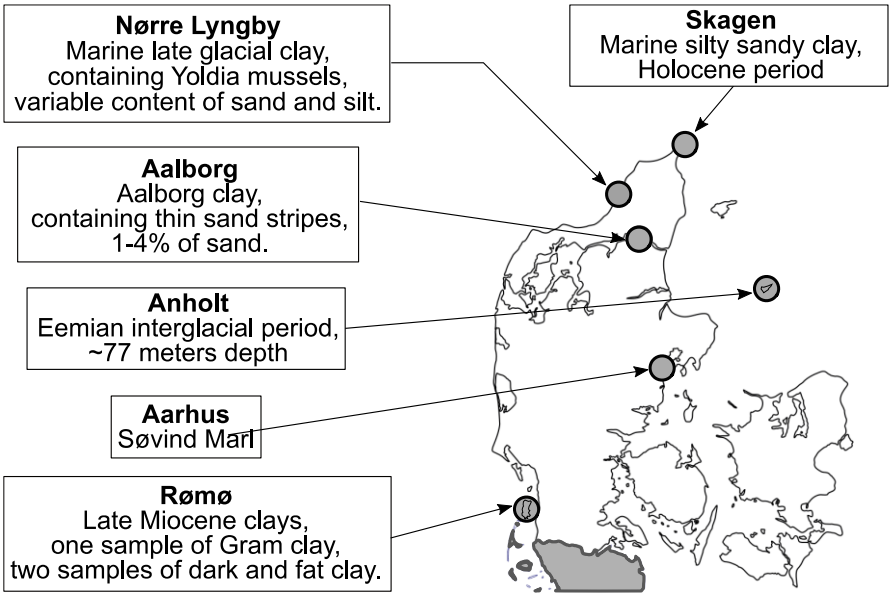

Fig. 10. Original sites of the clay samples.

CHAPTER 4. STATE OF THE ART

4.1. INTERPRETATION OF CONSOLIDATION AND CREEP

As anticipated in Section 1.2, settlement of a saturated soil deposit consists of two phases, a first primary consolidation, followed by a secondary consolidation phase. It is important to stress that the time of consolidation of a laboratory sample differs from the one of an in situ deposit. While a sample completes the dissipation of excess pore water pressure in few minutes, the soil deposit can take decades to dissipate the water; generally, the strain rates developed under an embankment are smaller than the ones generated in a laboratory test. To predict correctly the settlement in the field, it is necessary to define the creep process. Ladd et al. (1977) proposed two opposite creep theories. The first theory, so-called Hypothesis A, considers primary consolidation and creep two separate processes, where the end of primary (EOP) strain is not dependent on the consolidation time, so it is the same in the laboratory as in the field. Hypothesis A is experimentally supported by G. Mesri (2003). The second theory, Hypothesis B, implies that the EOP strain increases with the duration of primary consolidation, it includes a creep contribution in the primary consolidation, and it is supported by Serge Leroueil (2006). According to Hypothesis B, the EOP strain increases with the consolidation period, and the EOP strain in the field is higher than the one predicted by Hypothesis A (see Fig. 11). Several works were published in support of Hypothesis A (Mesri, 2009; Mesri and Vardhanabhuti, 2006) and Hypothesis B (Crawford, 1986; Degago et al., 2011; Imai et al., 2003). Hypotheses A and B can be represented on a set of isotache (Bjerrum, 1967; Šuklje, 1957), lines that have the same strain rate in the log(σ')-e diagram, as in Fig. 12. The isotache model represents the compressibility of soil by a system of parallel timelines and shows the uniqueness of the relationship between time, stress and void ratio (or strain).

Several methods separate the strains between primary consolidation and creep. Each of these methods presents different interpretations of the creep process. The commonly used 24 hours method consists of considering as consolidation strain the strain happening in the first 24 hours of each load step in an ILO test. Brinch Hansen (1961) proposed a graphical identification of the strains; the consolidation strain is linear when represented on the $\sqrt{t}$-e plane, while the creep strain is linear on the log(t)-e plane. Taylor (1948) suggested the square root of the time fitting method, which represents the strains on a $\sqrt{t}$-e plane. The so-called Anaconda method is based on Jacobsen's interpretation of creep and, among the methods applied, is the only one considering primary consolidation and creep two processes not separated (Jacobsen, 1992a). Paper C, applying these methods to clay samples, evaluates their influence on the compression curve and the determination of preconsolidation stress. Another way to separate the consolidation and creep strains is according to the strain rate $\frac{\partial \varepsilon}{\partial t}$. By defining the strain rate associated with the EOP state, the corresponding strain defines

the compression curve. For clays that reach the EOP before 24 hours, the desired value of strain rate varies between $5x10^{-8}$ s^{-1} for low compressibility clays and 10^{-7} s^{-1} for high compressibility clays (Leroueil, 2006).

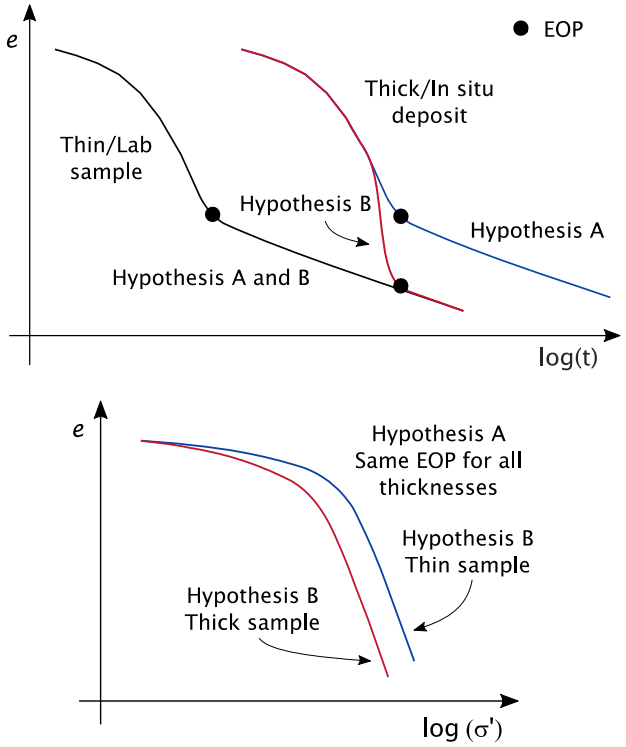

Fig. 11. Influence of sample thickness according to Hypotheses A and B.

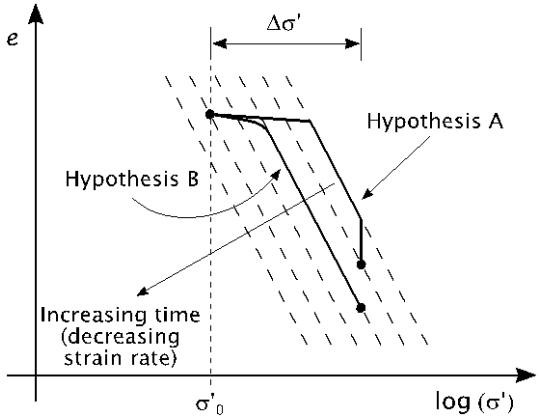

Fig. 12. Representation of Hypotheses A and B on the isotache lines after Serge Leroueil (2006).

4.2. EFFECT OF SAMPLE DISTURBANCE

Preserving the original soil structure in a sample is one of the main challenges of laboratory testing. Only an undisturbed sample can guarantee the correct evaluation of soil properties, stress-strain and strength behaviour. The sample disturbance induces destruction of the soil, leading to a decrease in preconsolidation stress and C_c and an increase in C_s (Leroueil and Hight, 2003; Lim et al., 2018). Several causes lead to sample disturbance (Ladd and Degroot, 2003). The disturbance of a sample can be due to sampling operation, transportation, adopted equipment and original sample depth. A long-term storage period contributes to the sample disturbance and reduces undrained shear strength and preconsolidation stress (Helene A Amundsen et al., 2015). Sample preparation (handling, trimming), and the swelling due to the contact with the saturated porous stones, can cause sample disturbance. A more rounded compression curve characterises a poor quality sample, compared to the one of an undisturbed sample (see Fig. 13).

It is important to define the degree of sample disturbance to have an understanding of the reliability of results. Lunne et al. (1997) suggested a procedure commonly adopted to describe the sample quality and based on tests on marine clays. The method by Lunne et al. calculates the ratio $\Delta e/e_0$ (where e_0 is the initial void ratio, and Δe is the change between e_0 and the void ratio corresponding to the in situ stress) to classify the degree of disturbance among four categories (Table 1).

Other criteria assessing the sample disturbance exist. For example, the one suggested by Karlsrud and Hernandez-Martinez (2013), which evaluates the trend of M. The best performance of this method is returned when it is applied on CRS tests, because of the higher amount of data points compared to ILO tests. The sample quality is not univocally defined: evaluating the disturbance with different criteria can change the quality rating (Helene Alexandra Amundsen et al., 2015).

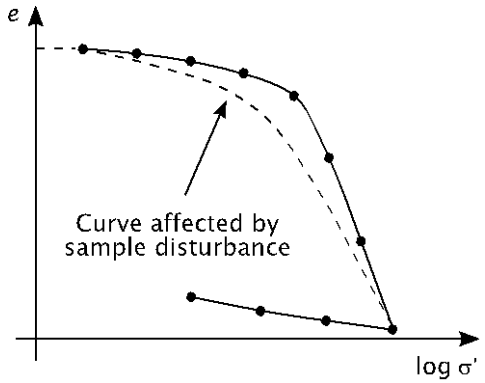

Fig. 13. Sketch of a compression curve affected by sample disturbance.

Table 1. Sample quality based on $\Delta e/e_0$ from oedometer tests taking into account the OCR (after Lunne et al. 1997).

Sample quality	**$\Delta e/e_0$ OCR 1-2**	**$\Delta e/e_0$ OCR 2-4**
Very good to excellent (1)	<0.04	<0.03
Good to fair (2)	0.04-0.07	0.03-0.05
Poor (3)	0.07-0.14	0.05-0.10
Very poor (4)	>0.14	>0.10

4.3. DEFORMATION PROPERTIES INVESTIGATED THROUGH OEDOMETER TESTING

Oedometer testing provides deformation properties useful to define the consolidation and creep processes of the soil tested. The following paragraphs list the stiffness and permeability parameters interpreted through the different papers.

4.3.1. COMPRESSION AND RECOMPRESSION INDEXES

As anticipated in Section 1.3, the compression curve returns the compression index, $C_c = \Delta e/\Delta\log(\sigma')$, and the recompression index, $C_r = \Delta e/\Delta\log(\sigma')$. While C_r relates to soil settlements for loads before the preconsolidation stress σ'_p, C_c relates to the virgin compression curve and loads higher than the σ'_p. C_c and C_r are parameters of constitutive soil models that define the stiffness of soft soils. Alternatively, the stiffness is also represented in terms of λ^* (4.1) and κ^* (4.2), which refer to the compression curve in the plane $\ln(\sigma')$–ε.

$$\lambda^* = \frac{C_c}{2.3(1 + \mathrm{e}_0)} \tag{4.1}$$

$$\kappa^* \approx \frac{2C_r}{2.3(1 + \mathrm{e}_0)} \tag{4.2}$$

4.3.2. COMPRESSIBILITY RATIO AND CONSOLIDATION MODULUS

The compressibility ratio m_v is the volume decrease per increase of effective pressure during compression (4.3). The primary consolidation settlements can be computed as in equation (4.4).

$$m_v = \frac{\Delta\varepsilon_v}{\Delta\sigma'} \tag{4.3}$$

$$S = \int_0^H m_v \cdot \Delta\sigma' \cdot dz \tag{4.4}$$

The soil compressibility is represented by the oedometer modulus or consolidation modulus M (4.5), reciprocate of m_v. The modulus M is a stress-dependent stiffness parameter.

$$M = \frac{\Delta\sigma'}{\Delta\varepsilon_v} \tag{4.5}$$

4.3.3. PERMEABILITY *K*

The coefficient c_v (4.6) can be related to the ratio between the permeability k and the compressibility ratio m_v by the volume weight of water γ_w.

$$c_v = \frac{k_v}{m_v \cdot \gamma_w} \tag{4.6}$$

4.3.4. SECONDARY COMPRESSION INDEX C_α

The secondary settlements continue at a decreasing rate over the life span of the structure. The creep contribution is relatively small in clays, but it can be the major deformation contribution in organic soil. It is possible to determine the secondary compression index C_α in the log*(t)-e* curve (see Fig. 14). Usually, C_α is calculated over a single log cycle (4.7). Mesri and Godlewski (1977) observed that the ratio C_α/C_c is between 0.025 and 0.10 for different kinds of soil and typically 0.037 for inorganic clays. The secondary settlements S_s in the field can be calculated as in equation (4.8).

$$C_\alpha = \frac{\Delta e}{\log\frac{t_2}{t_1}} \tag{4.7}$$

$$S_s = \frac{H_0}{1 + e_{EOP}} C_\alpha \log\frac{t_s}{t_{pc}} \tag{4.8}$$

where H_0 = thickness of the soil deposit to be evaluated after excavation, but before loading, e_{EOP} = void ratio corresponding to complete primary consolidation in the test specimen, t_s = time considered for the calculation of secondary compression, t_{pc} = time to complete primary consolidation in the consolidating soil deposit in the field.

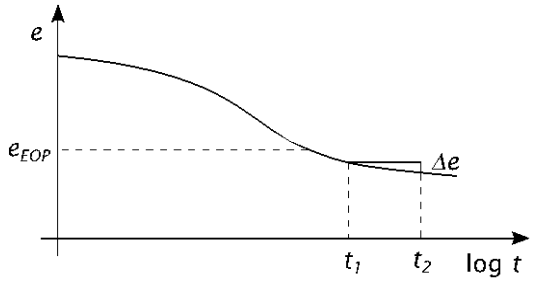

Fig. 14. Determination of C_α in the log(t)-e plane.

Alternatively, as for the C_c and C_r indexes, C_α is also represented with the term μ^*, which refers to the curve in the plane ln(t)–ε.

$$\mu^* = \frac{C_\alpha}{2.3(1+e_0)} \tag{4.9}$$

4.3.5. PRECONSOLIDATION PRESSURE σ'_P

The identification of σ'_p is important for the calculation of settlements and the interpretation of subsequent correlated parameters. Among them, for example, the undrained shear strength, as discussed by Skempton (1954) or by the SHANSEP method (Ladd and Foott, 1974), and the overconsolidation ratio *OCR* (σ'_p/σ'_{vo}).

There are several methods to interpret σ'_p from an oedometer test. All of them assume that the soil changes stiffness in the zone where the σ'_p belongs, from a stiffer to a softer behaviour. Some interpretations directly rely on the compression curve and a graphical construction based on it; others evaluate a secondary parameter. In the first group, there are the methods developed by Casagrande (1936), Pacheco Silva (1970), Jacobsen (1992b) and the bi-logarithmic methods by Butterfield (1979), Oikawa (1987), Onitsuka et al. (1995). Other methods, relying on a subsequent parameter, are, for example, the one proposed by Janbu (1969), interpreting the modulus *M*, or the work criterion by Becker et al. (1987), or the interpretation of C_α by Akai (1960). Not all the interpretations are designed for all kinds of soft soil. For example, Jacobsen (1992b) proposed an empirical method based on the results of oedometer tests on overconsolidated marine Danish clay.

It is worth mentioning that the compression curve plotted on a semi-logarithmic plane has been considered in the past an inaccurate representation of soil behaviour (Janbu, 1969; Wesley, 2019). Wesley (2019) criticizes the fact that, on this plane, all the different soils appear to behave in the same bilinear way; the log scale is a reasonable representation only for soft normally consolidated sedimentary clays, while, for the other soils, the arithmetic plot is recommended.

The preconsolidation pressure, defined as the point where the compression curve bends, is more generally defined as yield stress or quasi-preconsolidation stress because the bending of the curve can also be caused by structural changes in the soil, like alteration of clay mineral, cementation, or aging (Augustensen et al., 2004; Bjerrum, 1967; Liingaard et al., 2004; Ma et al., 2014). Leonards and Ramiah (1960) termed the apparent preconsolidation stress due to such effects as the quasi-preconsolidation pressure, and Leonards and Deschamps (1995) stressed the influence of a long period of secondary compression in the development of the quasi-preconsolidation stress (see Fig. 15).

This discussion wants to highlight the fact that the preconsolidation pressure is time-dependent, and it is related to the adopted strain rate (Augustensen et al., 2004; Leroueil et al., 1985). According to the isotache model, a system of parallel lines in the log(σ')-e plane represents a unique relationship between void, strain rate and stress. When an ILO test is performed, an increasing load increment duration causes the position of the virgin compression line to translate downwards (Graham et al., 1983) (see Fig. 16). In the same way, a decrease in strain rate in CRS oedometer leads to a decrease in σ'_p (Crawford, 1965). Therefore, the σ'_p determination relies also on the conditions a test is performed, not only to the interpretation theory applied.

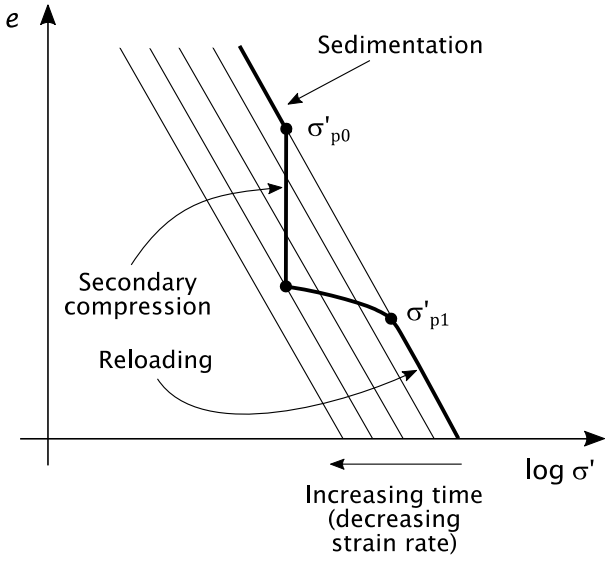

Fig. 15. Development of quasi-preconsolidation due to secondary compression.

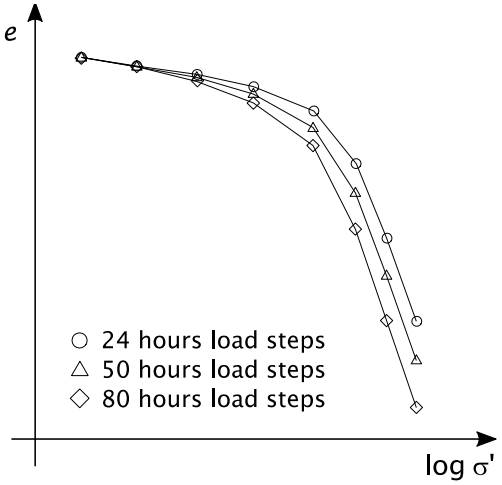

Fig. 16. An increasing load step duration shifts a compression curve downwards.

4.4. ILO AND CONSTANT RATE OF STRAIN OEDOMETER TEST

Even if this research does not present results from the Constant Rate of Strain oedometer testing, it is worth mentioning this kind of procedure in relationship with the ILO test. While the ILO test is a stress control test, a CRS test is performed not by applying incremental loads, but it is a continuous test during which the strain rate $\dot{\varepsilon}_p$ is constant.

Hamilton and Crawford (1959), Smith and Wahls (1969), Wissa et al. (1971) developed the CRS oedometer testing method to remedy the disadvantages of ILO testing. Some of the weaknesses of the ILO are the long testing time, the widely spaced data points that make it difficult to define σ'_p, and the variable amount of creep taken into account in the different load steps (Leroueil et al., 1983). The main advantages of the CRS test in comparison with ILO tests are the possibility to obtain a continuous (less scattered) log(σ')-*e* curve and to reduce the testing time.

The choice of the $\dot{\varepsilon}_p$ is the major variable in a CRS test, and the most appropriate $\dot{\varepsilon}_p$ to adopt is unknown a priori. A too high strain rate (fast CRS test) leads to the development of pore water pressure; on the other hand, a low strain rate returns a log(σ')-*e* curve including secondary deformations. The choice of an appropriate $\dot{\varepsilon}_p$ is based on prior ILO tests or following the Unified Soil Classification System, as suggested by ASTM D4186 (2012). The procedures that derive $\dot{\varepsilon}_p$ from ILO results rely on the quality of the ILO test (Mesri and Feng, 2018, 1986; Ozer et al., 2012). As an example, equation (4.10) is the relationship proposed by Mesri and Feng (1986) to find the axial strain rate $\dot{\varepsilon}_p$, associated to EOP state and expected to produce nearly zero excess pore pressure.

$$\dot{\varepsilon}_p = \frac{k_{v0}}{2^{C_c/C_k} H^2} \frac{\sigma'_p}{\gamma_w} \frac{C_\alpha}{C_c} \tag{4.10}$$

where k_{v0} is the initial permeability of the specimen, and H is its maximum drainage distance.

Some authors, after the choice of a proper $\dot{\varepsilon}_p$, presented test programs where the CRS results are in good agreement with the EOP compression curves from ILO tests (Andries et al., 2019; Mesri and Feng, 2018, 1986; Moozhikkal et al., 2019; Ozer et al., 2012). Fig. 17 shows different results for St. Hilaire clay from Mesri and Feng, (2018), where the compression curve from a CRS oedometer test is compared to the compression curve from an ILO test.

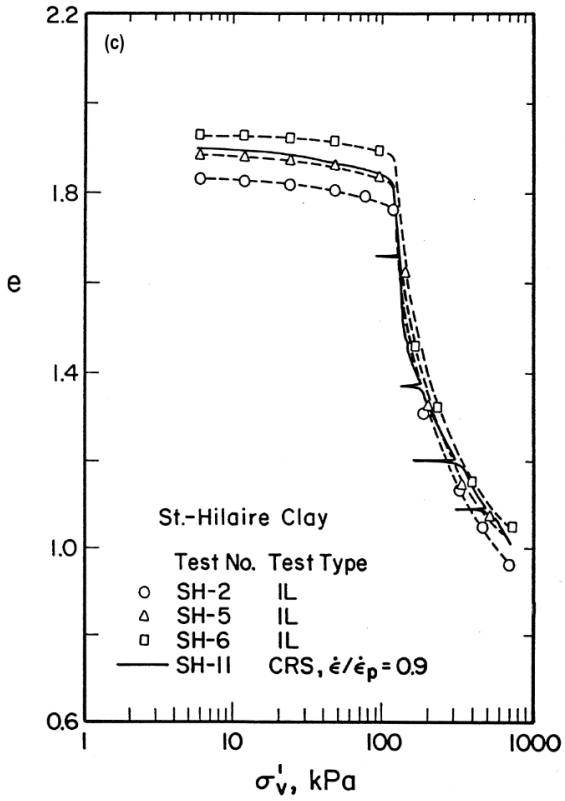

Fig. 17. A compression curve from a CRS test compared to the EOP curves from ILO tests (Mesri and Feng, 2018).

4.5. EXPANSIVE SOILS AND SWELL PRESSURE

Expansive soils are soils that expand or shrink when water is added or when they dry out, respectively. Two phenomena causing a volume alteration in soils are, for example, the seasonal dry and wet cycles and the movement of the groundwater table. Expansive soils can cause different damages to structures, as cracks on basement floors and walls.

Expansive soils swell because they contain swelling clay minerals, for example, montmorillonite and bentonite (Foster, 1954; Norrish, 1954). The swelling process presents two phases, not distinct clearly; the first phase is an initial crystalline phase, which is followed by an osmotic phase (Slade et al., 1991). Crystalline swelling happens because clay minerals, having a concentration of cations near the surface, attract water molecules. Osmotic swelling (or diffuse double layer swelling) occurs at inter-layer separations because of the presence of cations between the soil particles. Besides the soil minerals, other factors have an impact on the swelling potential and influence the swell behaviour: initial dry density, initial water content, confining pressure and cry-wetting history (Buzzi et al., 2011; Seed et al., 1961; Tripathy et al., 2002).

4.5.1. OEDOMETER TESTING AND HEAVE PREDICTION METHODS

A proper design can predict the soil heave due to the swell, and oedometer testing is the most accepted method to quantify the swelling potential. Two are the oedometer procedures commonly applied to identify the swelling pressure. One is the Consolidation-Swell (CS) test, and the second one is the Constant-Volume (CV) test. During a CS test, the sample firstly swells loaded by the inundation stress σ'_i (stress under which the sample is inundated by water), after it is loaded through several steps to reach its initial height again. The pressure corresponding to this height is the so-called consolidation swell pressure σ'_{cs}. During a CV test, the sample volume is kept constant under the effect of vertical stress that prevents the sample from swelling and varies during the time. The highest registered pressure is the constant-volume swelling pressure σ'_{cv}. These two methods are schematically represented in Fig. 18. The value of σ'_{cv} is lower than the value of σ'_{cs}; this is because it is easier to prevent the sample from swelling than to compress it back to the original height (Nelson et al., 2015).

The prediction of the heave is a fundamental step in the design of shallow and deep foundations in expansive soils. The calculation of the heave can be based on empirical or oedometer test methods. The oedometer methods rely on results from CV and CS tests. Nelson et al. (2006) calculated the heave starting from the definition of the heave index C_H (4.11). The percent swell ε_s at a particular value of σ'_i and the σ'_{cv} are both needed to determine C_H. Common geotechnical engineering practice is running only the CS test, and only the CS swelling pressure is measured. There are empirical relationships that return the value σ'_{cv}, for example, the ones suggested by Thompson

et al. (2006) or by John D. Nelson and Chao (2014). From Fig. 18, the strain in the layer can be written as:

$$\frac{\varepsilon_{s\%}}{100} = C_H \cdot \log\frac{\sigma'_{cv}}{\sigma'_i} \tag{4.11}$$

Using the definition of C_H above, J. D. Nelson et al. (2006) calculated the heave of a soil layer as:

$$\Delta H = C_H \cdot H \cdot \log\frac{\sigma'_{cv}}{\sigma'_f} \tag{4.12}$$

where H is the thickness of the soil layer, and the final vertical net normal stress σ'_f replaces the inundation stress σ'_i in equation (4.11). The value σ'_f is calculated from the weight of the soil layers above the swelling deposit and the self-weight of the structure. Vanapalli and Lu (2012) describe other heave prediction methods.

ASTM D4546-08 suggests an inundation period between 24 and 72 hours. Instead, it is not precisely defined how long a sample should be allowed to swell in a CS test (or prevented to swell in a CV test) to make the sample develop its full swelling potential. This time varies from one soil to another. The increase of swelling pressure at a decreasing rate was shown by Seed et al. (1961). Previous experimental investigation shows that a sample of highly plastic claystone still exhibits swelling potential after 40 days (Nelson, 2015).

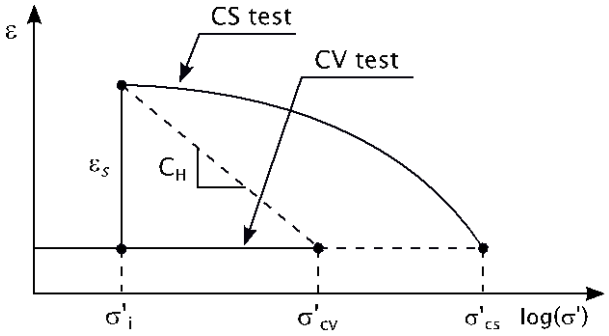

Fig. 18. Schematic procedure for CV and CS tests.

4.6. NUMERICAL MODELLING

Paper E focuses on the representation of soft soil by three different constitutive soil models. Oedometer tests are numerically validated in Plaxis with the Hardening Soil model, the Soft Soil Creep model and the Creep-1CLAY1S model, which features are summed up in the next paragraphs.

Soil shows a non-linear, time-dependent and often anisotropic behaviour. Many constitutive models describe the different aspects of soil behaviour in a more or less sophisticated way. The more complicated is a model, the more input parameters are needed. There is often a lack of laboratory or in situ tests to get the input parameters, and it is necessary to derive indirectly part of them. The selection of a soil model compromises between an accurate representation of the soil and the number of tests available. Choosing a soil model depends on the dominant load situation, for example, a tunnelling problem involves primarily the unloading, and therefore it is important to select a model able to represent this condition. Brinkgrere (2005) presents an overview of the tests needed to derive (directly or indirectly) the strength and deformation parameters; the ILO test is the one that allows the most complete derivation of stiffness parameters. After the constitutive model is selected and the parameters derived, it is important to evaluate the performance of the "artificial soil", i.e., the chosen soil model with the input parameters (Brinkgreve and Engin, 2013). The test validation permits to compare the laboratory results and the model result, but also to calibrate the parameters to have the best fit.

4.6.1. HARDENING SOIL MODEL

The Hardening Soil model (Schanz et al., 1999) can simulate both soft and stiff soils. In contrast to the simpler Mohr-Coulomb model, plastic behaviour in the Hardening Soil (HS) model can occur before failure, and the yield surface can expand due to plastic straining. The HS model permits plastic strain due to deviatoric loading and compression, it has stress-dependent stiffness, permits soil dilatancy and follows the Mohr-Coulomb failure criterion (defined by parameters c, φ, ψ). In the p-q plane, the elastic region of the HS model is closed by a shear hardening yield surface and a cap yield surface, which intersects the p axis at stress equal to the isotropic preconsolidation stress p_p (see Fig. 19).

Limitations of the HS model are the impossibility to reproduce creep and softening behaviour and to represent hysteresis in cyclic loading and difficulties in representing very soft soil with $E_{50} > 2E_{oed}$. Kharaghani et al. (2018) investigate the performance of the HS model on simulating soft soil and finds a good agreement for test validation on Bangkok clay.

From an ILO test, it is possible to directly determine the stiffness parameters E_{eod} (tangent stiffness for primary oedometer loading), and E_{ur} (unloading / reloading stiffness) through their alternatives λ^*, κ^*; and indirectly E_{50} (secant stiffness in

standard drained triaxial test). It may be possible to find the K_0 directly if the horizontal stresses have been measured while performing an ILO.

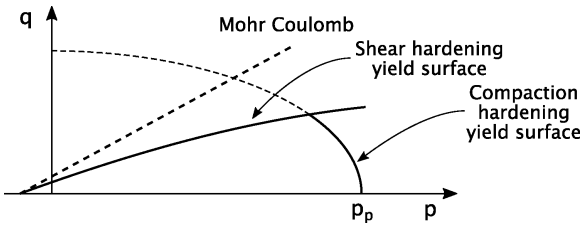

Fig. 19. Yield surfaces for the HS model.

4.6.2. SOFT SOIL CREEP MODEL

As the HS model, the Soft Soil Creep (SSC) model presents stress-dependent stiffness, expanding yield surface and failure according to the Mohr-Coulomb criterion. However, it considers time-dependent deformation, and it can simulate isotache behaviour following Hypothesis B. The SSC model (Vermeer and Neher, 1999) assumes that all the plastic strains are time-dependent and that the preconsolidation stress increases with the longer a sample is left to creep. The SSC model adopts the yield surface from the Modified Cam-Clay model (see Fig. 20), which expands to the right side and an associated flow rule, meaning that the plastic strain increment is perpendicular to the yield surface. The value p^{eq} is a generalized stress calculated by using the critical state line slope M, as in equation (4.13), and p_p^{eq} is a generalized equivalent preconsolidation stress. The creep strain depends on the stiffness parameter described in Section 4.3, and on p_p^{eq}. Relevant creep strains are calculated only when $p^{eq} > p_p^{eq}$. The SSC model should be limited to situations where the compression is the main loading conditions. Another limitation is the fact that the creep rate is considered constant with stress level and time, while, in reality, it is a decreasing value.

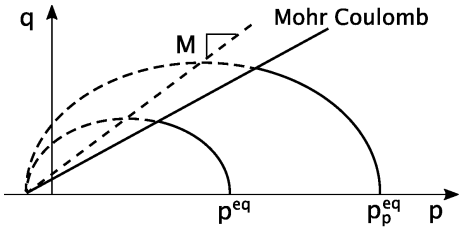

Fig. 20. Yield surfaces of the SSC model.

$$p^{eq} = p + \frac{q^2}{M^2 \cdot (p + c \cdot cot\varphi)} \tag{4.13}$$

$$\dot{\varepsilon_v}^c = \frac{\mu^*}{\tau}\left(\frac{p'^{eq}}{p'^{eq}_p}\right)^{\frac{\lambda^*-k^*}{\mu^*}} \frac{\partial p'^{eq}}{\partial p'} \tag{4.14}$$

4.6.3. CREEP-1CLAY1S MODEL

Among the models applied in Paper E, the Creep-1CLAY1S model (Sivasithamparam et al., 2015, 2013) is the most advanced, it can simulate creep, anisotropic behaviour and bonding. To model the presented clays, this research ignored anisotropy and bonding. By neglecting these two phenomena, the creep formulation in the Creep-1CLAY1S model is the same as in the SSC model, and the plastic deformation is only time-dependent. In the *p-q* plane (see Fig. 21), the strain increments are based on the Normal Consolidation Surface (NCS) and the Current Stress Surface (CSS), and they follow an associated flow rule. The surface is rotated at an angle α, the degree of initial anisotropy, which, if it is equal to zero, represents isotropic behaviour. The Creep-1CLAY1S model is a complicated model that includes many features here not investigated; this research uses this model as a term of comparison with the SSC for the long term deformation.

This model requires deriving intrinsic stiffness parameters from a sample that has lost any bonding. To do so, remoulded samples should be used to get intrinsic modified compression index λ_i* and intrinsic modified creep index μ_i*. This would require additional laboratory work. Another option is to calculate intrinsic values from tests where very high stresses were applied; however, in this case, there is uncertainty about the level of stress needed to erase the sample structure, and this can lead to inaccuracies.

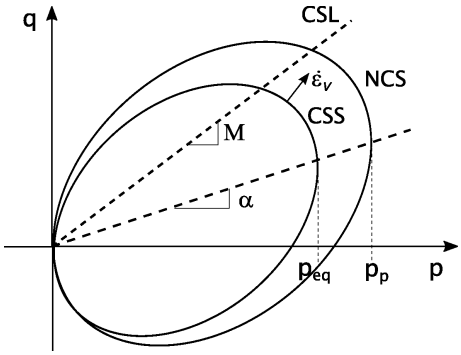

Fig. 21. NCS and CSS of the Creep-1CLAY1S model.

CHAPTER 5. METHOD

This thesis project presents the results of ILO tests and CV swelling tests performed on different Danish soils. The oedometer testing procedure has been shortly presented in Section 1.3, and Section 5.1 describes the two oedometer equipment used in the test programs: the oedometer with a floating ring and the automatic oedometer with a fixed ring. Section 5.2 presents a summary of the experimental program and an overview of the sample preparations. Finally, Section 5.3 describes the interpretation and correction applied to the CV swelling tests on the Søvind Marl samples.

5.1. ILO OEDOMETER EQUIPMENT

This project presents the results obtained by using two kinds of oedometer equipment. One is the automatic oedometer, which applies stress through a mechanical pressure-controlled system (see Fig. 22). This tool does not require placing the weight manually; after the user inserts the load sequence in the computer program, the test starts and the transition between a load step to the next one is automatic. During each load step, the contact between the head cap and the sample surface is constant since the controllers follow the sample settlement with a displacement accuracy equal to 0.2%. A fixed ring 4 mm thick confines the sample, and the maximum load applied is equal to 10 kN. The automatic oedometer is the equipment also employed to perform the constant volume swelling tests presented in this thesis. The mechanical pressure head kept constant the height of the sample, preventing it from swelling, while the transducers recorded the swelling pressure applied to the pressure head by the sample.

The second oedometer employed is the so-called AAU oedometer developed at Aalborg University. This equipment is inspired by the oedometer designed by Moust Jacobsen (Jacobsen, 1970) and shown in Fig. 23. The AAU oedometer (see Fig. 24) aims to reduce the inaccuracy stemming from the deformations of the equipment itself. The load is applied through a dead weight, and it is transferred firstly to a ball and after to the head cap. The maximum applicable load is equal to 27.5 kN; this makes it possible to apply high stresses to the sample. A floating ring of 1.5 cm thickness confines the sample and moves downwards during the loading, following the sample's displacement. This characteristic should minimize the friction between the soil sample and the ring.

Fig. 22. Automatic oedometer.

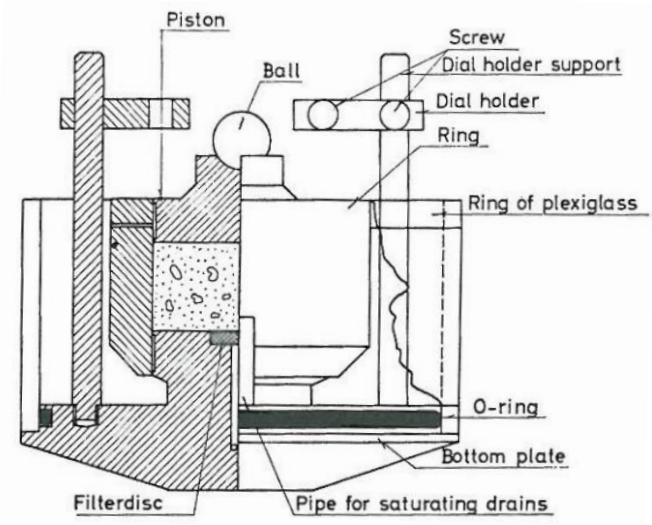

Fig. 23. The oedometer designed by Moust Jacobsen, Jacobsen (1970).

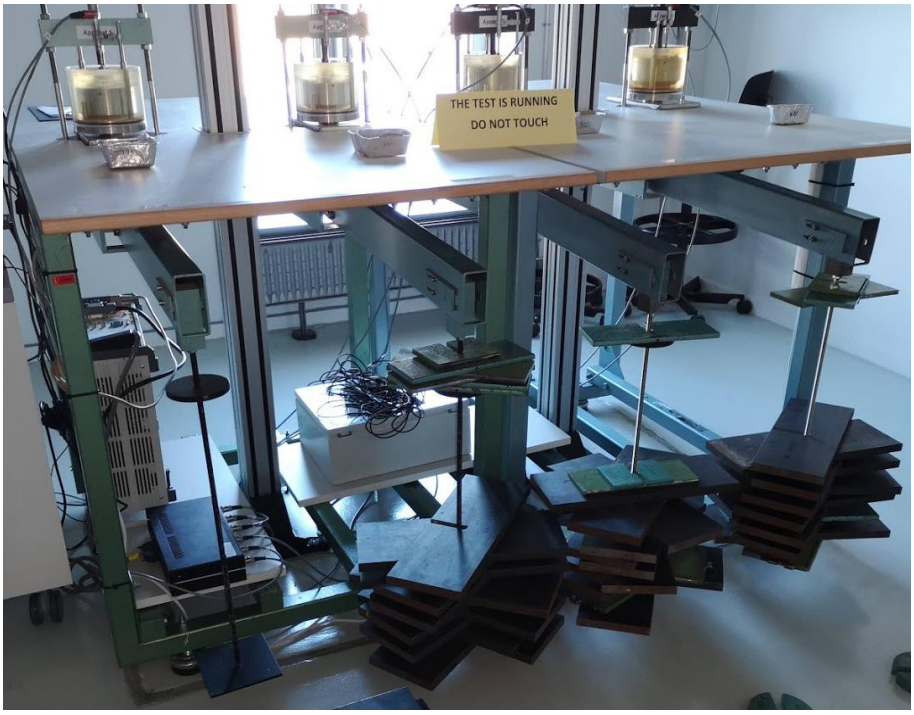

Fig. 24. AAU oedometers with applied dead weights.

5.2. TEST PROGRAM OVERVIEW

5.2.1. THE CHALK INVESTIGATION

The experimental program began with ILO tests on chalk (Paper B). The preparation of chalk samples started from rough blocks excavated mechanically and collected in the Aalborg Portland chalk pit. The sample preparation proved to be challenging and time-consuming (Nielsen et al., 2019), and several attempts were made before finding the most efficient preparation method. The first method consisted of placing a cylindrical ring directly on the block of chalk and pressing it down. The core sample inside this ring was pushed into the consolidation ring afterward. This procedure showed a low rate of success, and many cracks developed on the sample surface, especially when attempting to prepare samples of 70mm in diameter. A second procedure started with a drilling phase employing a hole saw cutter, followed by a pressing phase, when the sample was pushed into the oedometer ring. Finally, the sample surface was levelled by hand through a smooth blade. The second procedure proved to be the most successful, thanks to the hole saw cutter holding the sample and preventing the crack formation during the pressing phase. The chalk preparation was the most time consuming, and it implied the roughest manipulation of the samples. At the end of the preparation phase, nine ILO samples were ready to be tested in both the

oedometer equipment. A test counted about 16-18 load steps and each single load step lasted one week.

5.2.2. UNDISTURBED CLAY SAMPLES

Papers A, C and D present some results of clay samples tested during the Ph.D. project, and some results coming from a database of samples previously tested at the AAU laboratory. To the first group belong the samples of Aalborg clay, Søvind Marl and remoulded clay from Vejle.

The core samples of the clays tested were collected through a rotary tube and stored in plastic tubes afterward. Before testing, the samples were hand-trimmed and fit into the oedometer rings. Swelling during sampling and at the beginning of the test, and desiccation during the storage period are among the factors that can cause sample disturbance. Paper A and Paper E evaluate the degree of disturbance of the clay samples according to the Lunne criteria (Lunne et al., 1997). In the example in Fig. 25, the sample disturbance is evaluated for an oedometer test on a marine clay from Nørre Lyngby. Given an in situ stress equal to 220 kPa, the degree of sample disturbance is equal to $\Delta e/e_0$= 0.055. Considering that the sample has an OCR between 1 and 2, the quality category is equal to 2.

While Paper C applied different separation of strains methods, Paper A represented the compression curves by selecting the void ratio corresponding to a strain rate equal to 5 x 10^{-8} s^{-1} for each load step. By doing so, the compression curve does not take into account the creep. Exceptions were the compression curves of Søvind Marl samples, which took into account the full strain developed during the 24-hours step since the consolidation process is slower in comparison to the other clays.

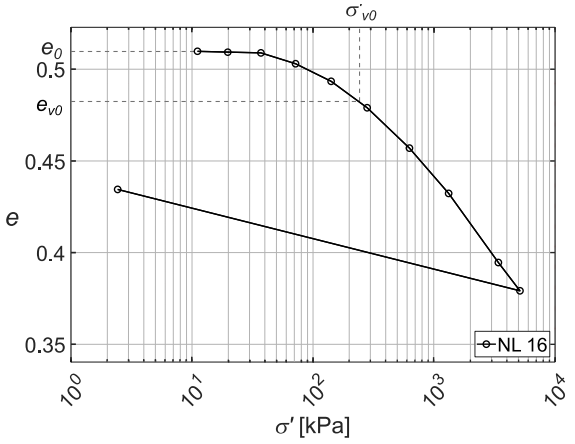

Fig. 25. Evaluation of sample disturbance on a Nørre Lyngby clay by Lunne et al. criteria.

5.2.3. REMOULDED CLAY SAMPLES

Paper A presents the results of nine validation tests on remoulded clay. To remould the samples, the clay was mechanically mixed at a water content equal to 25%. The clay slurry filled some block forms with dimensions 5x10x20cm. After a storage period, the oedometer ring was pushed into the clay block and the sample levelled by hand. This validation program involved both the automatic and AAU oedometer. An initial load (100, 250, 500, or 1000 kPa) was applied for two weeks. When it was removed, a swelling happened and it did not cause the sample to reach a void ratio larger than the initial one. Afterward, a standard ILO test started from 10 kPa. This investigation aimed to understand the correct method to identify the artificial "pre-applied" stress history. Seven validation tests doubled the consecutive load steps ($\Delta\sigma'=\sigma'$), while the other two counted intermediate steps ($\Delta\sigma'=0.5\sigma'$). As done for the undisturbed clay samples, the compression curves were drawn by selecting a strain rate equal to 5×10^{-8} s^{-1}.

5.3. INTERPRETATION OF SWELLING PRESSURE

Paper D evaluates the long term swelling pressure of Søvind Marl. Four constant volume swelling tests, followed by a standard ILO, were performed by the automatic oedometer equipment. Two CV swelling tests lasted 24 hours, and two CV swelling tests lasted 19 weeks. By doing so, it was possible to compare for two samples the value of σ'_{cv} at 24 hours with the σ'_{cv} over a longer period.

Besides the uncertainty about the time required to develop the full swell pressure, the sample disturbance introduces some ambiguities too. A disturbance to the soil structure can cause a reduction in matric suction, and this leads to an underestimation of σ'_{CV}. When an ILO test is run after a CV phase, different graphical correction methods can be applied to the compressibility curve. For example, the method suggested by Fredlund et al. (2012) is a graphical construction based on the point of maximum curvature in the compression curve. Nelson and Miller (1992) proposed a second graphical method. On the log(σ')-*e* plane, a horizontal line is drawn passing through the estimated uncorrected $(\sigma'_{CV})_U$. Afterward, a tangent to the virgin compression line is added. The intersection between these two lines is the corrected value of swelling pressure $(\sigma'_{CV})_C$. The effect of this kind of correction can be remarkable. Fredlund et al. (2012) showed a corrected swelling pressure 300% higher than the uncorrected one. John D. Nelson et al. (2015) found out that the difference can be around 100% for highly overconsolidated clays, and the higher is the estimated swelling pressure, the greater the effect of the correction. It is important to stress how these methods, based on graphical constructions, heavily rely on the quality of the ILO test. When tangents to the maximum point of curvature or tangents to the virgin curve are drawn, the amount of load steps plays an important role in the result of the correction.

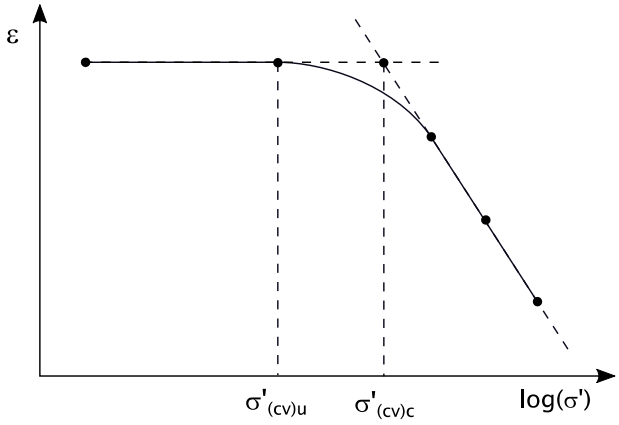

Fig. 26. Correction method by Nelson and Miller (1992).

CHAPTER 6. SUMMARY OF RESEARCH

This chapter is based on the results of the five papers collected in the thesis. The following paragraphs present the specific objectives achieved and show some of the papers' key figures.

Different soils show different compression behaviour, affected by soil initial state, stress history, stress path and time. The followed laboratory methodology plays an important role in the evaluation of the deformation properties as well. The oedometer testing is a widespread method carried out to identify the consolidation and creep properties of a soil, and traditionally, this procedure involves double loading and load steps lasting 24 hours. However, when interpreting oedometer results, it is necessary to keep in mind that deformation properties are time-dependent and strongly affected by laboratory procedure, as, for example, preconsolidation pressure, compression and secondary compression indexes and swelling pressure. Therefore, for a specific soil, it is worth developing a testing procedure that allows getting the best out of the often limited number of soil samples available. After the laboratory results are complete, other factors affect the final understanding of a soil behaviour, like the interpretation chosen to elaborate the data. This study shows, for example, that not every theory interpreting the preconsolidation stress suits every soil; and the swelling pressure, as a direct result of a constant volume swelling test, risks to underestimate the swelling potential if the value is not corrected.

The initial part of the experimental program consisted of four ILO tests on Aalborg clays samples carried out in the AAU equipment. The aim of this investigation was to understand what the most representative interpretative methodology for this specific clay is. More specifically, the scope of these tests was to investigate the effect of different separation of strains theories on the compression curve, and afterwards, on the preconsolidation stress determination. In a first phase, the separation of strains between consolidation and creep strain was achieved by four different theories, i.e., 24 hours, Brinch-Hansen, Taylor and ANACONDA theories. In a second phase, the preconsolidation stress was found for every compression curve through Akai, Janbu and Jacobsen's methods. Three additional samples of Yoldia clay from Nørre Lyngby underwent the same two-phases process. Both the two clays lead to the same conclusions. The application of different separation of strains methods does not show any relevant change in the compression curve nor the resulting preconsolidation pressure. However, it is evident how considering the consolidation over after 24 hours overestimates the consolidation time. In opposition, the choice of preconsolidation pressure theory largely affects the preconsolidation pressure. Jacobsen's construction predicts a preconsolidation pressure larger than the one interpreted through Akai and

Janbu's theories, in some cases, even more than the double. Some sources of error influencing the separation of strain methods and definition of preconsolidation pressure are the personal judgment and experience of the user, and, in general, an inaccurate laboratory practice. Peri et al. (2019), i.e., Paper C in this thesis, presents the results of ILO on Aalborg and Yoldia clays, which gave the opportunity to begin a discussion on the determination of preconsolidation pressure σ'_p in Danish clays.

The determination of σ'_p encounters several issues that make it difficult to define σ'_p as a clear and unique value. The value σ'_p is affected by subjective interpretation and the interpretative theory chosen. Moreover, σ'_p is time-dependent and strictly influenced by the followed laboratory methodology. In fact, it is known that the longer a load step lasts, the smaller is the value of σ'_p and vice versa. Finally, a poor sample quality complicates further the identification of a clear σ'_p on the compression curve. The results of fourteen ILO tests on medium-stiff Danish clays are analysed with the purpose to understand what is the optimal interpretation methodology that returns the most accurate value of σ'_p. The samples originate from Rømø, Anholt, Aalborg, Nørre Lyngby and Aarhus. They differ for initial in situ stress, void ratio, water content and degree of disturbance, which is defined according to the criteria by Lunne et al. (1997). To draw the compression curve, a unique value of strain rate was selected for each sample, i.e., the compression curves are represented by the EOP void ratio for every load step. The σ'_p interpretative theories applied are both graphical (Onitsuka, Pacheco-Silva and Jacobsen's theories) and based on a parameter related to σ'_p (Janbu and Becker's theories). In addition to the results of undisturbed samples, this part of the study includes the interpretation of σ'_p on nine remoulded clay samples from Vejle. These are validation tests with an artificial pre-applied σ'_p. The scope was finding out which theories return the σ'_p closest to the pre-applied one. It is possible to draw some considerations on the interpretative theories applicability from the results of the fourteen Danish clays. For example, the Jacobsen's theory, an empirical formula calibrated only on results of overconsolidated marine clays, is not meaningful for other kinds of clays. The Onitsuka's theory does not perform correctly on a compression curve without a clear bilinear trend. In general, the Jacobsen's theory tends to overestimate σ'_p, and the best agreement is found between the Onitsuka and Becker's theories. The Janbu's theory is often the most difficult to apply. The results on the undisturbed samples show a relationship between σ'_p and initial void ratio, and a relationship between σ'_p and dispersion of the σ'_p from different theories. Large variability in the σ'_p determination is due to the chosen interpretative theory (see Fig. 27). Fig. 27 shows that, for most of the samples, the average resulting σ'_p decreases for higher e_0. For higher level of sample disturbance, there is a larger dispersion of σ'_p. The validation tests on remoulded clay confirm the difficulties in applying the Janbu's theory and the similarity between the σ'_p evaluated by Becker and Onitsuka (see Fig. 28). The validation test results also show how all the applied interpretative theories generally overestimate the artificial pre-applied σ'_p. Moreover, the reduction of the load increment ratio, for example, from $\Delta\sigma'=\sigma'$ to $\Delta\sigma'=0.5\sigma'$, would benefit both the graphical methods and the interpretations based on a subsequent parameter.

This work is included in Peri et al. (2020c), called Paper A in this thesis. The same paper includes also a discussion about the determination of Søvind Marl, a Paleogene clay studied further during the PhD because of its high swelling potential.

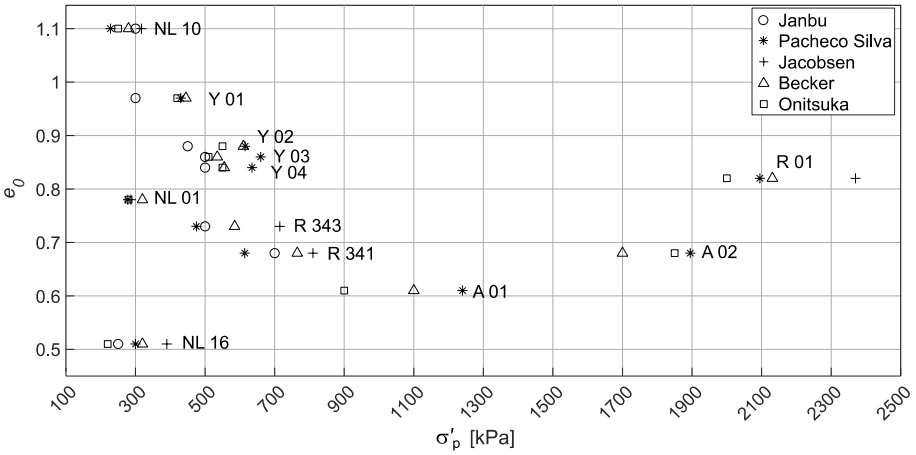

Fig. 27: Void ratio e_0 and preconsolidation stresses σ'_p for clays from Nørre Lyngby, Aalborg, Anholt and Rømø, from Peri, Zwanenburg, et al. (2020c).

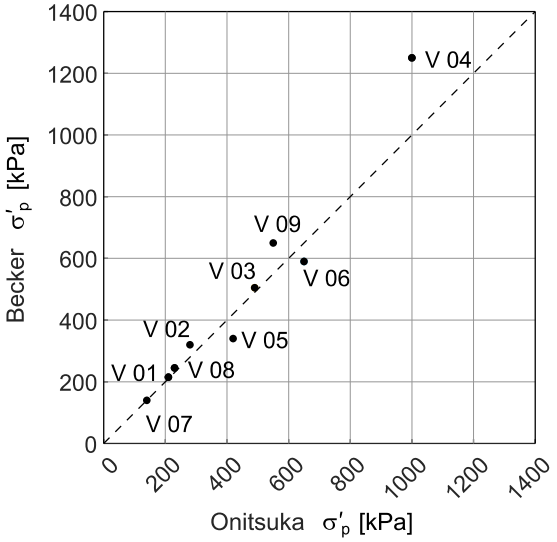

Fig. 28: Results of Becker and Onitsuka et al. interpretations for the validation tests on remoulded clay, from Peri, Zwanenburg, et al. (2020c).

Besides its characteristic “loss of memory” and high plasticity, the Søvind Marl presents high swelling potential. Four samples of Søvind Marl were tested in the automatic oedometer. The samples underwent a constant volume swelling test, followed by an ILO test. For two samples taken at 63 meters depth, the CV swelling test lasted 24 hours (Test 1 and 2), for the other two samples, originating from 35 meters depth, the CV test lasted about 19 weeks (Test 3 and 4). Over the 19 weeks of the CV tests, Test 3 and 4 show a swelling potential constantly developing. Even though the value of σ'_{cv} seems constant after one day, it keeps increasing at a lower rate until five weeks (see Fig. 29). The change between the swelling pressure at 24 hours and the maximum σ'_{cv}, equal to about 270 kPa, is 30-38% for the two tests. Tests 1 and 2 present lower σ'_{cv} values (about 30 and 80 kPa) compared to the 24 hours σ'_{cv} in Tests 3 and 4. A swelling test lasting almost five months is not realistic in the engineering practice. However, the development of σ'_{cv} over the CV test stresses the importance of following the evolution of the swelling pressure while the test runs. If there are already some data available showing that the examined soil exhibits high swelling potential, a compromise could be running, for example, a one-week test and adding 20% to σ'_{cv}. Besides the underestimation of swelling potential due to the shortening of laboratory time, errors in the σ'_{cv} estimation stem from the sample disturbance during sampling. To overcome this problem, the graphical construction by Nelson and Miller (1992) is applied, and the initial σ'_{cv} is almost doubled. This correction relies on the quality of the compression curve, and it is made difficult by the typical not clearly bilinear behaviour of Søvind Marl. The correction can be helped by having a less scattered curve, i.e., by applying more load steps, and by starting the ILO test with a stress close to the σ'_{cv}. This work is included in Peri et al. (2021), called Paper D in this thesis.

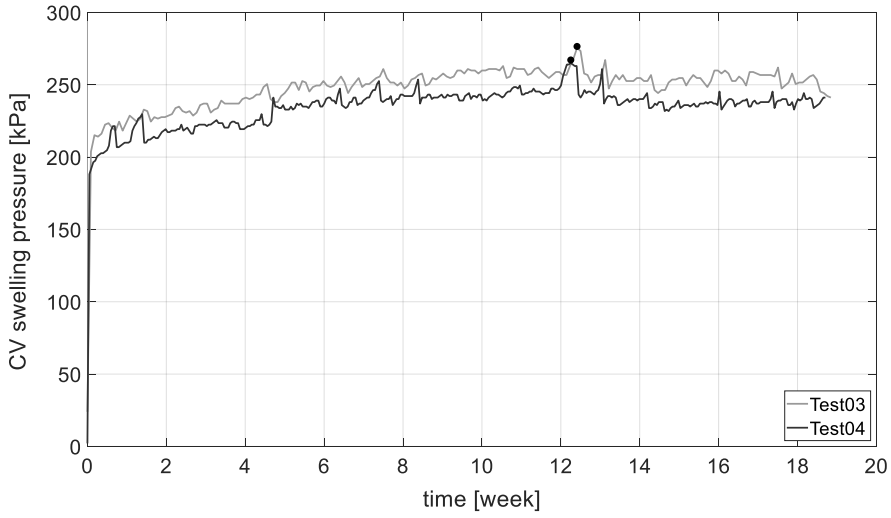

Fig. 29: Swelling pressure development over 19 weeks, from Peri et al. (2021).

As for clay, each kind of chalk presents specific behaviour. This project only evaluates the compressive behaviour of Rørdal chalk, a stiff soil found in the North Sea basin. Among the prepared soil samples, the chalk proved to be the most difficult material to deal with, and many attempts were made in order to have high quality samples. This part of the project presents a reliable procedure to prepare chalk samples for oedometer test from blocks. Results of ILO tests, run both in the automatic and AAU oedometer, and the precautions needed to achieve the optimal methodology are presented in Peri et al. (2020b), called Paper B in this thesis. Reliable oedometer results are guaranteed only by applying stresses high enough to reach the virgin compression curve. Moreover, each load step should run long enough to identify the complete long-term behaviour. Therefore, the load steps lasted one-week. This lengthy procedure (about five months for each test) makes it possible to complete the consolidation and to identify three strain contributions. The three strain contributions that compose the chalk deformation under constant load are an initial crushing, a consolidation strain and a creep strain. The initial crushing is due to grain crushing or progressive pore breakdown, and its estimation helps to predict the settlements during the construction phase. Thanks to the one-week steps, it is possible to clearly evaluate the creep contribution for this material (see Fig. 30), which it is important because chalk's long-term deformation is relevant for understanding the collapse of oil fields in chalk reservoirs. Among the three strains, the crushing and creep strains account for about 6% of the total strain, where the creep is the minor contribution. To draw the compression curves accounting only for the consolidation strains, the crushing is filtered manually, and the creep is filtered by the ANACONDA method. A comparison between the different compression curves shows large variability in the final deformation and the necessity of applying high loads not to underestimate both the σ'_p and the compression index.

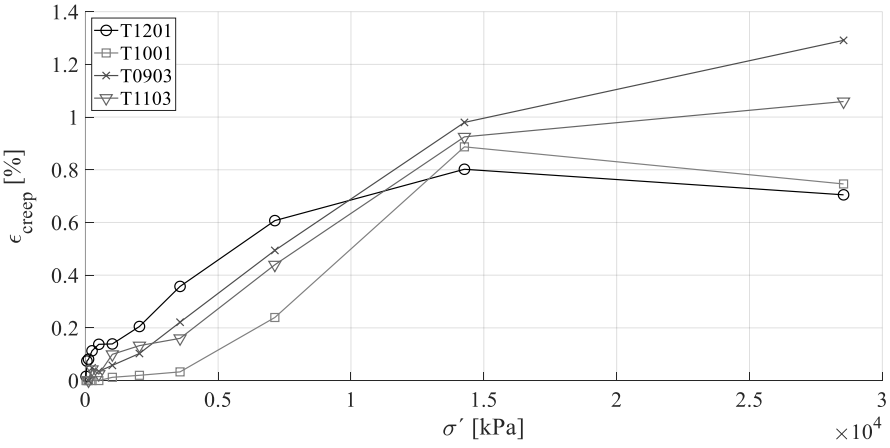

Fig. 30: Rørdal chalk creep strains under the loading applied by the AAU oedometer, from Peri et al. (2020b).

When the experimental program ended, a numerical investigation took place. The FEM program used is the commercial software Plaxis 2D. This part of the project highlights the importance of a test validation, which permits to select a suitable constitutive soil model and to calibrate the soil parameters. If there is not a good fit between the laboratory curve and simulated curve, it is impossible to assume that the "artificial soil" is ready to simulate a real situation in a more complicated model. The validated samples originate from Anholt, Nørre Lyngby and Skagen. These medium-stiff Danish clay samples differ for initial in situ stress, OCR, void ratio, water content and degree of disturbance, which is defined according to the criteria by Lunne et al. (1997). Three constitutive soil models are employed: Hardening Soil, Soft Soil Creep and isotropic Creep-1CLAY1S models. Altogether, the three soil models return a final deformation very similar to the laboratory results. The SSC model returns the best fit for the NC clay samples, and the HS model suits the presented clays since they are not too soft. The Creep-1CLAY1S model tends to overestimate the deformation in the recompression curve and the stiffness during the unloading for all the samples; therefore, it is not the model to be chosen in a situation with expected swelling. Besides the correct definition of the deformation properties, this study shows the effects of the vertical and horizontal permeability and the change of permeability with void ratio c_k. The smaller the permeability and the change in permeability of a deposit, the smaller are the settlements (see Fig. 31). The relationship $c_k \approx 0.15 \sim 0.3 e_0$ fits the tested samples. The simulation of a sand embankment over a clay deposit investigates the long-term settlement predictions for the three soil models, the influence that some input parameters have on that prediction and the development of pore pressure over 1370 days (the construction time plus consolidation periods). As for the validation of oedometer tests, the Creep-SClay1S model and the SSC model predict the largest and smallest final settlement, respectively. While the κ^* and μ^* parameters have the largest influence, the permeability parameters k_v and k_h have a secondary effect, and c_k does not show any relevant change in the final settlement prediction of this kind of application. The pore pressure excess development shows how the consolidation process is faster for the SSC model than for the other two (see Fig. 32), meaning that the HS and Creep-SClay1S models will still develop some further settlements after the final 1000 days of consolidation. This work is included in Peri et al. (2020a), called Paper E in this thesis.

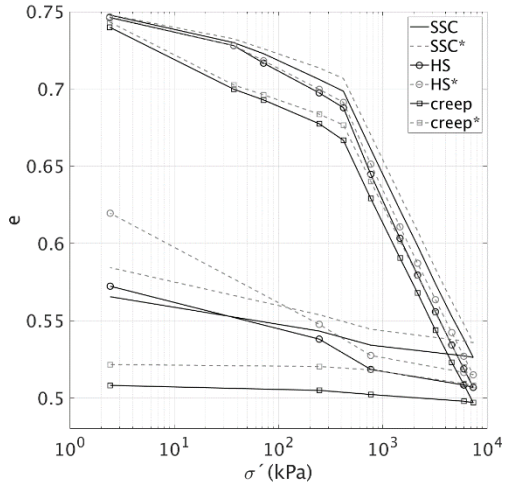

Fig. 31: Evaluation of the permeability influence for different soil models, from Peri, Koteras, et al. (2020a).

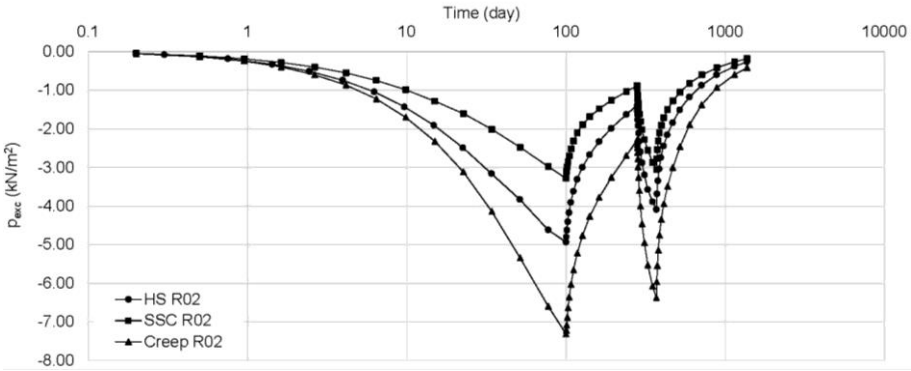

Fig. 32. Development of excess pore pressure, p_{exc}, for soil NLR02, from Peri, Koteras, et al. (2020a).

CHAPTER 7. CONCLUSION

The results presented in this Ph.D. thesis show the compression behaviour of a set of Danish clays and chalk, particularly concerning laboratory procedure, interpretation of results and influence of testing time. This research highlights the consequences of laboratory procedure and interpretation of oedometer testing on deformation and stiffness parameters. Laboratory results and interpretation of different Danish soils confirmed how each soil needs special attention and specific laboratory testing procedure. What is the influence of ILO test methodology on chalk compressive behaviour? What is the time a tertiary highly plastic clay takes to develop its full swelling potential? Can different constitutive soil models represent medium-stiff Danish clays? These are some of the questions this project answered. This chapter presents the general final considerations drawn during this Ph.D. project.

This Ph.D. thesis stresses the importance of correct execution and interpretation of oedometer testing. The different experimental results showed that generic laboratory procedures and saving testing time could lead to inaccurate and poor quality data. No shortcut can provide the same data quality as a test program designed for specific soil and run for a time long enough to define the complete parameters. For example, this was proven in the case of empirical formulas to derive C_c and C_α, used in case of lack of data, that could lead to inaccurate parameters for soil modeling. On the other hand, it is not realistic to assume that a laboratory facility, performing numerous analyses, can run an oedometer test or a swelling test lasting months. Therefore, the solution is to find a compromise between time and accuracy; for instance, by inspecting the output of a test while the test is still running, and not just relying on the standard procedure. This rule can be applied to several aspects of oedometer testing, for example, to each load step in an ILO, to establish the end of the consolidation; or to draw the compression curve progressively, checking if the virgin compression line is well defined; or to a swelling pressure test, where the swelling potential is evolving during the time. By introducing these measures, a test runs enough time to fully develop the searched features, for example, swelling potential or long-term settlements, and, at the same time, the test is not extended further.

It is known that some soils require steps lasting longer than 24 hours to reach the creep, and others complete the consolidation in a shorter period. Even if the different separation of strain methods did not lead to a noticeable difference in representing the EOP compression curve, they show how a 24 hours long-lasting load step in an ILO is an approximated procedure that cannot be applied to every soil. To overcome these ambiguities, a valid separation of strains was achieved by the identification of a unique strain rate at which the consolidation ends. This procedure requires inspecting carefully the time-deformation curve, but, in comparison to the other methods, permits to save some time during the interpretation and it is less subjective.

The results of different preconsolidation pressure interpretations highlight how varying can be the identification of this parameter. The dependency on the testing procedure (as seen in the case of Rørdal chalk), the testing time, the initial void ratio (as seen for different clays) and the applied interpretative method are all attributes of the preconsolidation pressure and need to be kept in mind. Moreover, the preconsolidation pressure is not always a univocal value, as seen, for example, in the case of the Søvind Marl. The obtained wide range of preconsolidation pressure for each sample suggests applying more than one interpretative method. An option, in the case of medium-stiff clays like the ones investigated in the thesis, could be applying both Becker and Onitsuka et al. interpretations. These methods provide a fast interpretation and are often in agreement with each other. The way a test is performed affects the choice of the method to be applied. It is noted, for example, how compression curves with few points in the recompression line were difficult to interpret by a bi-logarithmic construction.

The simulations of ILO tests carried out in Plaxis underlined the importance of validating a laboratory test. A complete representation of the sample, with its boundaries and real size, allows the selection of the most suitable soil constitutive model and the calibration of the deformation parameters, even in case of some input are just approximated (for example, the strength parameters in Paper E). It is advised to simulate the test by using more than one soil model, but not to limit the definition of the artificial soil only to a validation model on a laboratory scale. In fact, studying the artificial soil in a complete application permits understanding the soil model's performance in terms of long-term development of creep and excess pore pressure.

7.1. RECOMMENDATIONS FOR FUTURE RESEARCH

The results found have raised several questions that future research could answer.

1. A testing program with more samples of Søvind Marl could clarify if the swelling potential depends on depth. Some consolidation-swell tests, in addition to the constant volume swelling tests, could expand the knowledge about swelling behaviour and the heave index C_H for highly plastic clays.
2. A wider range of remoulded clay samples with different pre-applied preconsolidation pressure could be tested. In this way, it might be possible to clarify if the applicability and variability of the preconsolidation pressure interpretative theories depend on the preconsolidation stress value.
3. A deeper investigation of the Creep-1CLAY1S model could expand the knowledge of this soil model not widely used yet. The definition of the intrinsic modified indexes (λ_i* and μ_i*), through the interpretation of remoulded samples, could evaluate the accuracy of the modified indexes obtained at very high stress. The full potential of the model could be achieved by the definition of the anisotropy and bonding parameters.

REFERENCES

Abrahamsen, N., Readman, P.W., 1980. Geomagnetic variations recorded in Older (> 23 000 B.P.) and Younger Yoldia Clay (14 000 B.P.) at Nørre Lyngby, Denmark. Geophys. J. 62, 329–344. https://doi.org/https://doi.org/10.1111/j.1365-246X.1980.tb04859.x

Akai, K., 1960. De strukturellen eigenschaften von schluff (The structural properties of silt).

Alam, M.M., Fabricius, I.L., Christensen, H.F., 2012. Static and dynamic effective stress coefficient of chalk. Geophysics 77, L1–L11. https://doi.org/10.1190/geo2010-0414.1

Amundsen, Helene A, Emdal, A., Sandven, R., Thakur, V., 2015. On engineering characterisation of a low plastic sensitive soft clay, in: 68th Annual Canadian Geotechnical Conference GeoQuébec. Quebec City, Canada.

Amundsen, Helene Alexandra, Thakur, V., Emdal, A., 2015. Comparison of two sample quality assessment methods applied to oedometer test results, in: Proc. of the 6th International Symposium on Deformation Characteristics of Geomaterials. pp. 923–930. https://doi.org/10.3233/978-1-61499-601-9-923

Andries, J., Verastegui, D., De Beule, K., Baertsoen, A., 2019. One-dimensional consolidation of overconsolidated clay using constant rate of strain testing, in: IS-Glasgow. Glasgow, United Kingdom, p. 02011. https://doi.org/10.1051/e3sconf/20199202011

ASTM D4546-08: Standard Test Methods for One-Dimensional Swell or Settlement Potential of Cohesive, 2008. https://doi.org/10.1520/D4546-08.2

Augustensen, A.H., Liingaard, M., Lade, P. V., 2004. Evaluation of time-dependent behavior of soils. Int. J. Geomech. 137–156. https://doi.org/10.1061/(ASCE)1532-3641(2004)4:3(137)

Becker, D.E., Crooks, J.H.A., Been, K., Jefferies, M.G., 1987. Work as a criterion for determining in situ and yield stresses in clays. Can. Geotech. J. 24, 549–564. https://doi.org/https://doi.org/10.1139/t87-070

Bjerrum, L., 1967. Engineering geology of Norwegian normally-consolidated marine clays as related to settlements of buildings. Géotechnique 17, 83–118. https://doi.org/https://doi.org/10.1680/geot.1967.17.2.83

Brinch Hansen, J., 1961. A model law for simultaneous primary and secondary

consolidation, in: Proceedings of the 5th International Conference on Soil Mechanics and Foundation Engineering. Paris, France, pp. 133–136.

Brinkgrere, R.B.J., 2005. Selection of soil models and parameters for geotechnical engineering application. Geo-Frontiers Congr. 2005 69–98. https://doi.org/10.1158/1538-7445.AM2013-1522

Brinkgreve, R.B.J., Engin, E., 2013. Validation of geotechnical finite element analysis, in: 18th International Conference on Soil Mechanics and Geotechnical Engineering. Paris, France, pp. 677–682.

Butterfield, R., 1979. A natural compression law for soils (an advance on e–log p′). Géotechnique 29, 469–480. https://doi.org/10.1680/geot.1979.29.4.469

Buzzi, O., Giacomini, A., Fityus, S., 2011. Towards a dimensionless description of soil swelling behaviour. Géotechnique 61, 271–277. https://doi.org/10.1680/geot.7.00194

Casagrande, A., 1936. The determination of pre-consolidation load and its practical significance, in: Proceedings of the 1st International Conference on Soil Mechanics and Foundation Engineering. pp. 60–64.

Crawford, C.B., 1986. State of the art: evaluation and interpretation of soil consolidation tests, in: Yong, R.N., Townsend, F.C. (Eds.), Consolidation of Soils: Testing and Evaluation, ASTM STP 892. American Society for Testing and Materials, Philadelphia, pp. 71–103.

Crawford, C.B., 1965. The resistance of soil structure to consolidation. Can. Geotech. J. 2, 90–115. https://doi.org/https://doi.org/10.1139/t65-010

Dahou, A., Shao, J.F., Bederiat, M., 1995. Experimental and numerical investigations on transient creep of porous chalk. Mech. Mater. 21, 147–158. https://doi.org/https://doi.org/10.1016/0167-6636(95)00004-6

Degago, S.A., Grimstad, G., Jostad, H.P., Nordal, S., Olsson, M., 2011. Use and misuse of the isotache concept with respect to creep hypotheses A and B. Géotechnique 61, 897–908. https://doi.org/10.1680/geot.9.P.112

Delage, P., Schroeder, C., Cui, Y.J., 1996. Subsidence and capillary effects in chalks. EUROCK 1996 - Predict. Perform. Rock Mech. Rock Eng. 1291–1298.

Fabricius, I.L., 2007. Chalk: Composition, diagenesis and physical properties. Bull. Geol. Soc. Denmark 55, 97–128.

Foster, M.D., 1954. The relation between composition and swelling in clays. Clays Clay Miner. 3, 205–220. https://doi.org/10.1346/ccmn.1954.0030117

Fredlund, D.G., Rahardjo, H., Fredlund, M.D., 2012. Unsaturated Soil Mechanics in Engineering Practice. John Wiley & Sons, New York, USA.

Graham, J., Crooks, J.H.A., Bell, A.L., 1983. Time effects on the stress-strain behaviour of natural soft clays. Géotechnique 33, 327–340. https://doi.org/10.1680/geot.1983.33.3.327

Grønbech, G.L., Ibsen, L.B., Nielsen, B.N., 2015a. Preconsolidation of Søvind Marl - a highly fissured Eocene clay. Geotech. Test. J. 38, 501–510. https://doi.org/10.1520/GTJ20140246

Grønbech, G.L., Nielsen, B.N., Ibsen, L.B., Stockmarr, P., 2015b. Geotechnical properties of Søvind Marl — a plastic Eocene clay. Can. Geotech. J. 52, 469–478. https://doi.org/10.1139/cgj-2014-0066

Håkansson, E., Bromley, R., Perch-Nielsen, K., 1974. Maastrichtian chalk of North-West Europe - a Pelagic shelf sediment, in: Hsü, K.J., Jenkyns, H.C. (Eds.), Pelagic Sediments: On Land and under the Sea. pp. 211–233. https://doi.org/10.2475/ajs.276.5.670

Hamilton, J.J., Crawford, C.B., 1959. Improved determination of preconsolidation pressure of a sensitive clay, in: American Society for Testing and Materials. Special Technical Publication No. 254. Philadelphia, pp. 254–271.

Heilmann-Clausen, C., 2010. Palæogen - Fra drivhus til kølehus. GeoViden 3, 2–11.

Heilmann-Clausen, C., Nielsen, O.B., Gersner, F., 1985. Lithostratigraphy and depositional environments in the Upper Paleocene and Eocene of Denmark. Bull. Geol. Soc. Denmark 33, 287–323.

Hjuler, M.L., Fabricius, I.L., 2009. Engineering properties of chalk related to diagenetic variations of Upper Cretaceous onshore and offshore chalk in the North Sea area. J. Pet. Sci. Eng. 68, 151–170. https://doi.org/https://doi.org/10.1016/j.petrol.2009.06.005

Homand, S., Shao, J.F.R., 2000. Mechanical behaviour of a porous chalk and Water/Chalk Interaction. Mech. Cohesive-Frictional Mater. 55, 583–606. https://doi.org/https://doi.org/10.2516/ogst:2000045

Imai, G., Tanaka, Y., Saegusa, H., 2003. One-dimensional consolidation modeling based on the isotach law for normally consolidated clays. Soils Found. 43, 173–

188. https://doi.org/https://doi.org/10.3208/sandf.43.4_173

International, A., 2012. ASTM D4186/D4186M: Standard Test Method for One-Dimensional Consolidation Properties of Saturated Cohesive Soils Using Controlled-Strain Loading.

ISO 17892-5:2017: Geotechnical investigation and testing - Laboratory testing of soil - Part 5: Incremental loading oedometer test, 2017.

Iversen, K.M., Nielsen, B.N., Augustensen, A.H., 2010. Strength Properties of Aalborg Clay. DCE Technical Reports, No. 92, Aalborg.

Jacobsen, M., 1992a. Karakteristiske belastningstilstande for moræneler (Characteristic stress conditions for clay till), in: 11th Nordic Geotechnical Meeting. Aalborg, Denmark, pp. 28–30.

Jacobsen, M., 1992b. Bestemmelse af forbelastningstryk i laboratoriet (Determination of preconsolidation stress in the laboratory), in: Proceedings of the 11th Nordic Geotechnical Meeting. Aalborg, Denmark, pp. 455–460.

Jacobsen, M., 1970. New oedometer and new triaxial apparatus for firm soils. Danish Geotech. Inst. Bull. 27, 7–20.

Janbu, N., 1969. The resistance concept applied to deformations of soils, in: Proceedings of the 7th International Conference on Soil Mechanics. pp. 191–196.

Japsen, P., 2000. Fra Kridthav til Vesterhav. Nordsøbassinets udvikling vurderet ud fra seismiske hastigheder (From the Cretaceous to the North Sea. The evolution of the North Sea basin is assessed on the basis of seismic velocities). Geol. Tidsskr. 2, 1–36.

Japsen, P., 1998. Regional velocity-depth anomalies, North Sea Chalk: A record of overpressure and Neogene uplift and erosion. Am. Assoc. Pet. Geol. 82, 2031–2074.

Kågeson-Loe, N.M., Jones, M.E., Petley, D.N., Leddra, M.J., 1993. Fabric evolution during the deformation of chalk. Int. J. Rock Mech. Min. Sci. Geomech. 30, 739–745. https://doi.org/https://doi.org/10.1016/0148-9062(93)90016-7

Karlsrud, K., Hernandez-Martinez, F.G., 2013. Strength and deformation properties of Norwegian clays from laboratory tests on high-quality block samples. Can. Geotech. J. 50, 1273–1293. https://doi.org/10.1139/cgj-2013-0298

Kharaghani, S., Bazaz, H.B., Rivard, P., Akhtarpour, A., 2018. A study on the efficiency of the hardening soil model for soft clay, in: 71st Canadian Geotechnical Conference. Edmonton, Canada.

Korsnes, R.I., Wersland, E., Austad, T., Madland, M.V., 2008. Anisotropy in chalk studied by rock mechanics. J. Pet. Sci. Eng. 62, 28–35. https://doi.org/https://doi.org/10.1016/j.petrol.2008.06.004

Krogsbøll, A., Hededal, O., Foged, N., 2012. Deformation properties of highly plastic fissured Palaeogene clay – Lack of stress memory ?, in: Proceedings of 16th Nordic Geotechnical Meeting. Copenhagen, Denmark, pp. 133–140.

Ladd, C.C., Degroot, D.J., 2003. Recommended practice for soft ground site characterization: Arthur Casagrande Lecture, in: 12th Panamerican Conference on Soil Mechanics and Geotechnical Engineering. Cambridge, MA, USA.

Ladd, C.C., Foott, R., 1974. New design procedure for stability of soft clays. J. Geotech. Eng. Div. ASCE 100, 763–786.

Ladd, C.C., Foott, R., Ishihara, K., Schlosser, F., Poulos, H.G., 1977. Stress - deformation and strength characteristics : state of the art report, in: 9th ICSMFE. Tokyo, Japan, pp. 421–494.

Lagerlund, E., Houmark-Nielsen, M., 1993. Timing and pattern of the last deglaciation in the Kattegat region, southwest Scandinavia. Boreas 22, 337–347. https://doi.org/https://doi.org/10.1111/j.1502-3885.1993.tb00195.x

Leonards, G.A., Deschamps, R.J., 1995. Origin and significance of the quasi-preconsolidation pressure in clay soils, in: Proceedings of International Symposium on Compression and Consolidation of Clayey Soils. Hiroshima, Japan, pp. 341–347.

Leonards, G.A., Ramiah, B.K., 1960. Time effects in the consolidation of clays. Pap. Soils 1959 Meet. 116–130. https://doi.org/https://doi.org/10.1520/STP44309S

Leroueil, S., 2006. The isotache approach. Where are we 50 years after its development by Professor Šuklje? (2006 Prof. Šuklje's Memorial Lecture), in: Proceedings of the 13th Danube-European Conference on Geotechnical Engineering. Ljubljana, Slovenia, pp. 55–88.

Leroueil, S., Hight, D.W., 2003. Behaviour and properties of natural soils and soft rocks, in: Tan, T.S., Phoon, K.K., Hight, D.W., Leroueil, S. (Eds.), Characterization and Engineering Properties of Natural Soils. A.A. Balkema Publishers, Tokyo, pp. 29–254.

Leroueil, S., Kabbaj, M., Tavenas, F., Bouchard, R., 1985. Stress–strain–strain rate relation for the compressibility of sensitive natural clays. Géotechnique 35, 159–180. https://doi.org/10.1680/geot.1985.35.2.159

Leroueil, S., Samson, L., Bozozuk, M., 1983. Laboratory and field determination of preconsolidation pressures at Gloucester. Can. Geotech. J. 20, 477–490. https://doi.org/https://doi.org/10.1139/t83-056

Leth, C.T., Andersen, J.D., Madsen, T., Larsen, K.A., 2016. Founding on (un)known chalk in Aalborg, in: Proc. of the 17th Nordic Geotechnical Meeting. Reykjavik, Iceland, pp. 249–256.

Liingaard, M., Augustesen, A., Lade, P. V., 2004. Characterization of models for time-Dependent behavior of soils. Int. J. Geomech. 4, 157–177. https://doi.org/10.1061/(asce)1532-3641(2004)4:3(157)

Lim, G.T., Pineda, J., Boukpeti, N., Carraro, J.A.H., Fourie, A., 2018. Effects of sampling disturbance in geotechnical design. Can. Geotech. J. 56, 275–289. https://doi.org/10.1139/cgj-2018-0016

Lunne, T., Berre, T., Strandvik, S., 1997. Sample disturbance effects in soft low plastic Norwegian clay, in: Proceedings of the Conference on Recent Developments in Soil and Pavement Mechanics. Rio de Janeiro, Brazil, pp. 81–102.

Ma, B., Muhunthan, B., Xie, X., 2014. Mechanisms of quasi-preconsolidation stress development in clays: A rheological model. Soils Found. https://doi.org/10.1016/j.sandf.2014.04.012

Maranini, E., Brignoli, M., 1999. Creep behaviour of a weak rock. Experimental characterization. Int. J. Rock Mech. Min. Sci. 36, 127–138. https://doi.org/https://doi.org/10.1016/S0148-9062(98)00171-5

Mesri, G., 2009. Effects of friction and thickness on long-term consolidation behavior of osaka bay clays. Soils Found. 49, 823–824. https://doi.org/10.3208/sandf.49.823

Mesri, G., 2003. Primary and secondary compression, in: Symposium on Soil Behavior and Soft Ground Construction. pp. 122–166.

Mesri, G., Feng, T.-W., 2018. Constant rate of strain consolidation testing of soft clays and fibrous peats. Can. Geotech. J. 56, 1526–1533.

Mesri, G., Feng, T.W., 1986. Stress–strain–strain rate relation for the compressibility

of sensitive natural clays, Discussion. Géotechnique 36, 283–290. https://doi.org/10.1680/geot.1986.36.2.283

Mesri, G., Godlewski, P.M., 1977. Time and stress compressibility interrelationships. J. Geotech. Eng. Div. 103, 417–430.

Mesri, G., Vardhanabhuti, B., 2006. Closure to "Secondary Compression" by G. Mesri and B. Vardhanabhuti. J. Geotech. Geoenvironmental Eng. 132, 817–818. https://doi.org/10.1061/(ASCE)1090-0241(2006)132

Moozhikkal, R., Sridhar, G., Robinson, R.G., 2019. Constant Rate of Strain Consolidation Test Using Conventional Fixed Ring Consolidation Cell. Indian Geotech. J. 49, 141–150. https://doi.org/10.1007/s40098-018-0299-1

Nelson, J.D., 2015. Time dependence of swelling in oedometer tests on expansive soil. 15th Asian Reg. Conf. Soil Mech. Geotech. Eng. 490–493. https://doi.org/10.3208/jgssp.OTH-35

Nelson, J.D., Chao, K.C., 2014. Relationship between swelling pressures determined by constant volume and consolidation-swell oedometer tests, in: Proceedings of the UNSAT2014 Conference on Unsaturated Soils. Sydney, Australia.

Nelson, J.D., Chao, K.C.G., Overton, D.D., Nelson, E.J., 2015. Oedometer Testing, in: Foundation Engineering for Expansive Soils. pp. 127–151. https://doi.org/10.1002/9781118996096.ch6

Nelson, J.D., Miller, D.J., 1992. Expansive Soils: Problems and Practice in Foundation and Pavement Engineering. John Wiley & Sons, New York.

Nelson, J.D., Reichler, D.K., Cumbers, J.M., 2006. Parameters for Heave Prediction by Oedometer Tests, in: 4th International Conference on Unsaturated Soils. Carefree, AZ, pp. 951–961.

Nielsen, O.B., 1995. Danmarks geologi fra kridt til i dag. Geologisk Institut, Aarhus Universitet, Aarhus, Denmark.

Nielsen, S.D., Peri, E., Nielsen, B.N., 2019. Evaluation of preparation techniques of chalk samples for oedometer testing, in: Proceedings of the XVII ECSMGE. Reykjavik, Iceland.

Norrish, K., 1954. The swelling of montmorillonite. Discuss. Faraday Soc. 18, 120–134.

Oikawa, H., 1987. Compression curve of soft soils. Soils Found. 27, 99–104.

https://doi.org/https://doi.org/10.3208/sandf1972.27.3_99

Okkels, N., Hansen, P.B., 2016. Swell pressure and yield stresses in Danish, highly overconsolidated, Palaeogene clays of extreme plasticity, in: Proceedings of the 17th Nordic Geotechnical Meeting. Reykjavik, Iceland, pp. 367–376.

Onitsuka, K., Hong, Z., Hara, Y., Yoshitake, S., 1995. Interpretation of oedometer test data for natural clays. Soils Found. 35, 61–70. https://doi.org/https://doi.org/10.3208/sandf.35.61

Ozer, A.T., Lawton, E.C., Bartlett, S.F., 2012. New method to determine proper strain rate for constant rate-of-strain consolidation tests. Can. Geotech. J. 49, 18–26. https://doi.org/10.1139/T11-086

Pacheco Silva, F., 1970. A new graphical construction for determination of the preconsolidation stress of a soil sample, in: Proceedings of the 4th Brazilian Conference on Soil Mechanics and Foundation Engineering. Rio de Janeiro, Brazil, pp. 225–232.

Peri, E., Bo Ibsen, L., Nordahl Nielsen, B., 2019. How to interpret consolidation and creep in Yoldia clay, in: 7th International Symposium on Deformation Characteristics of Geomaterials. EDP Sciences, Glasgow, United Kingdom. https://doi.org/10.1051/e3sconf/20199205005

Peri, E., Koteras, A., Damkilde, L., 2020a. Modelling the compressive behaviour of soft soil by validating laboratory results. Submitted to Geomech. Eng.

Peri, E., Nielsen, S.D., Nielsen, B.N., 2020b. Geotechnical recommendation for preparation, execution and interpretation of oedometer test on chalk. Submitted to Geotech. Geol. Eng.

Peri, E., Nielsen, S.D., Nielsen, B.N., Damkilde, L., 2021. Experimental evaluation of time effect on swelling pressure in high plasticity clay (In press), in: Proceedings of the Nordic Geotechnical Meeting 2020. Helsinki, Finland.

Peri, E., Zwanenburg, C., Damkilde, L., 2020c. Determination of preconsolidation pressure by different methods of interpretation. Submitted to Eng. Geol.

Piasecki, S., 1980. Dinoflagellate cyst stratigraphy of the Miocene Hodde and Gram formations, Denmark. Bull. Geol. Soc. Denmark 29, 53–76.

Richardt, N., 1996. Sedimentological examination of the Late Weichselian sea-level history following deglaciation of northern Denmark. Geol. Soc. Spec. Publ. 111, 261–273. https://doi.org/10.1144/GSL.SP.1996.111.01.17

Risnes, R., Flaageng, O., 1999. Mechanical properties of chalk with emphasis on chalk-fluid interactions and micromechanical aspects. Oil Gas Sci. Technol. 54, 751–758. https://doi.org/https://doi.org/10.2516/ogst:1999063

Schanz, T., Vermeer, P.A., Bonnier, P.G., 1999. The hardening soil model: Formulation and verification, in: Beyond 2000 in Computational Geotechnics. Ten Years of PLAXIS. Amsterdam, the Netherlands. https://doi.org/10.1201/9781315138206-27

Seed, H.B., Mitchell, J.K., Chan, C.K., 1961. Studies of swell and swell pressure characteristics of compacted clays. Highw. Res. Board Bull. 313, 12–39.

Sivasithamparam, N., Karstunen, M., Bonnier, P., 2015. Modelling creep behaviour of anisotropic soft soils. Comput. Geotech. 69, 46–57. https://doi.org/http://dx.doi.org/10.1016/j.compgeo.2015.04.015

Sivasithamparam, N., Karstunen, M., Brinkgreve, R.B.J., Bonnier, P.G., 2013. Comparison of two anisotropic creep models at element level, in: International Conference on Installation Effects in Geotechnical Engineering. Rotterdam, NL, pp. 72–78. https://doi.org/http://dx.doi.org/10.1201/b13890-12

Skempton, A.W., 1954. Discussion of the structure of inorganic soil, in: ASCE, Soil Mechanics and Foundation Division, 80 (478). pp. 19–22.

Slade, P.G., Quirk, J.P., Norrish, K., 1991. Crystalline swelling of smectite samples in concentrated NaCl solutions in relation to layer charge. Clay Clay Miner. 39, 234–238. https://doi.org/https://doi.org/10.1346/CCMN.1991.0390302

Smith, R.E., Wahls, H.E., 1969. Consolidation under constant rates of strain. J. Soil Mech. Found. Div. 95, 519–539.

Stenestad, E., 2006. Fluviokarst in the top of the Maastrichtian chalk at Rørdal, Northern Jutland, Denmark. Bull. Geol. Soc. Denmark 53, 93–110.

Strand, S., Hjuler, M.L., Torsvik, R., Pedersen, J.I., Madland, M. V., Austad, T., 2007. Wettability of chalk: impact of silica, clay content and mechanical properties. Pet. Geosci. 13, 69–80. https://doi.org/https://doi.org/10.1144/1354-079305-696

Šuklje, L., 1957. The analysis of the consolidation process by the isotaches method, in: Proceedings of the International Conference on Soil Mechanics and Foundaion Engineering. London, United Kingdom, pp. 200–206.

Taylor, D.W., 1948. Fundamentals of Soil Mechanics. John Wiley & Sons, New York,

USA.

Terzaghi, K., 1943. Theoretical Soil Mechanics. John Wiley & Sons. https://doi.org/10.1002/9780470172766

Thompson, R.W., Perko, H.A., Rethamel, W.D., 2006. Comparison of constant volume swell pressure and oedometer load-back pressure, in: 4th International Conference on Unsaturated Soils. Carefree, Arizona, United States, pp. 1787–1798. https://doi.org/10.1061/40802(189)150

Tripathy, S., Subba Rao, K.S., Fredlund, D.G., 2002. Water content - void ratio swell-shrink paths of compacted expansive soils. Can. Geotech. J. 39, 938–959. https://doi.org/10.1139/t02-022

Vanapalli, S.K., Lu, L., 2012. A state-of-the art review of 1-D heave prediction methods for expansive soils. Int. J. Geotech. Eng. 6, 15–41. https://doi.org/10.3328/IJGE.2012.06.01.15-41

Vermeer, P.A., Neher, H.P., 1999. A soft soil model that accounts for creep, in: Beyond 2000 in Computational Geotechnics. Ten Years of PLAXIS International. Amsterdam, pp. 249–261. https://doi.org/10.1201/9781315138206-24

Wesley, L.D., 2019. Genuine and false pre-consolidation and yield pressures, in: Proceedings of 7th International Symposium on Deformation Characteristics of Geomaterials. E3S Web of Conferences, Glasgow, United Kingdom. https://doi.org/10.1051/e3sconf/20199205001

Wissa, A.E.Z., Christian, J.T., Davis, E.H., Heiberg, S., 1971. Consolidation at constant rate of strain. Soil Mech. Found. Div. 97, 1393–1413.

APPENDIX

Søvind Marl

SM_01	e_0	= 1.168	H_0	= 35 mm	
	σ' (kPa)	e	eps %	time (h)	M (kPa)
	2.08	1.168	0	-	-
σ' cv	28.06	1.168	0	24	-
	300	1.15722194	0.49714286	24	54701
	600	1.11161342	2.60085714	24	14260
	1200	1.04269889	5.77957143	24	18876
	600	1.0485401	5.51014286	24	222694
	300	1.06016368	4.974	24	55955
	600	1.05522683	5.20171429	24	131744
	1200	1.0434453	5.74514286	24	110410
	2400	0.95659213	9.75128571	24	29954
	4800	0.80939422	16.5408571	24	35348
	2400	0.83513457	15.3535714	24	202142
	1200	0.87872066	13.3431429	24	59689
	2400	0.85568721	14.4055714	24	112949
	4800	0.79141221	17.3702857	24	80952
	10000	0.61160758	25.6638571	24	62699
	300	0.86482069	13.9842857	24	83051

Test SM_01

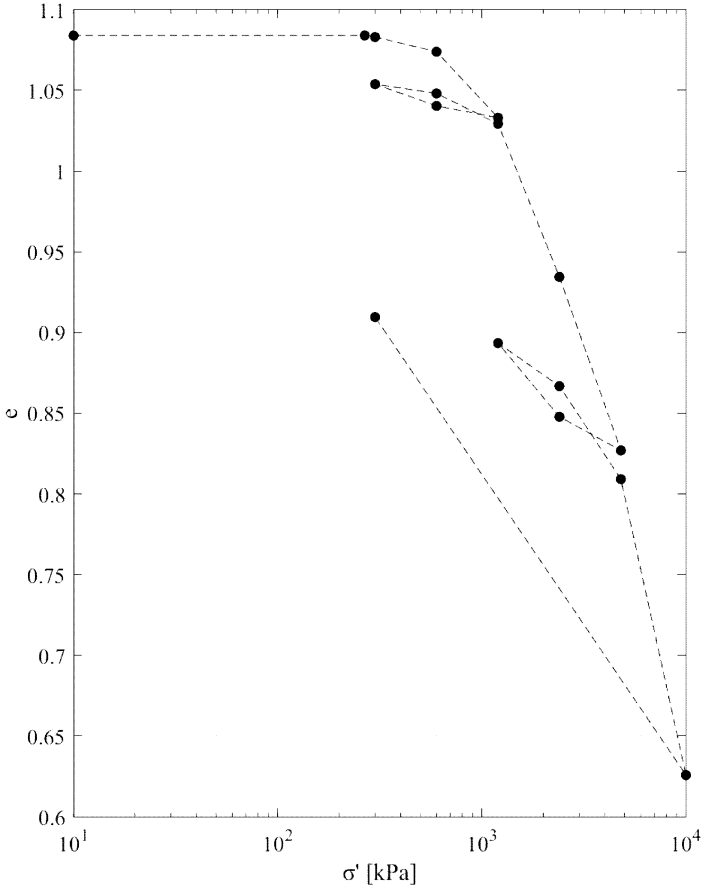

SM_02		e_0	= 1.143	H_0	= 35 mm
	σ' (kPa)	e	eps %	time (h)	M (kPa)
	2	1.143	0	-	-
σ' $_{CV}$	83	1.143	0	24	-
	300	1.12003622	1.07157143	24	20251
	600	1.07287798	3.27214286	24	13633
	1200	1.00871044	6.26642857	24	20038
	600	1.02038979	5.72142857	24	110092
	300	1.04195143	4.71528571	24	29817
	600	1.0340009	5.08628571	24	80863
	1200	1.00608985	6.38871429	24	46068
	2400	0.93252066	9.82171429	24	34955
	4800	0.79272053	16.3452857	24	36790
	2400	0.81981723	15.0808571	24	189809
	1200	0.86091997	13.1628571	24	62565
	2400	0.83696429	14.2807143	24	107348
	4800	0.77687151	17.0848571	24	85588
	10000	0.54402538	27.9502857	24	47858
	300	0.79763106	16.1161429	24	81966

Test SM_02

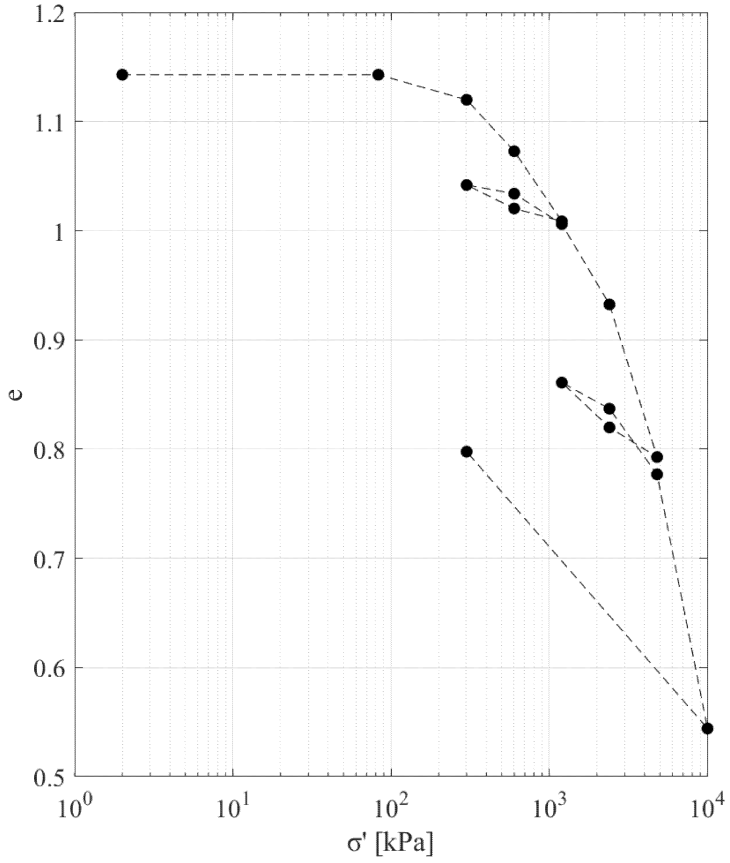

SM_03		e_0	= 1.1	H_0	= 35 mm
	σ' (kPa)	e	eps %	time (weeks)	M (kPa)
	10	1.1	0	-	-
σ' cv	276	1.1	0	18.85	-
	300	1.09928	0.03428571	2	70000
	600	1.0934	0.31428571	0.24	107143
	1200	1.01792	3.90857143	2	16693
	600	1.03058	3.30571429	2	99526
	300	1.05788	2.00571429	2	23077
	600	1.04558	2.59142857	2	51220
	1200	1.01462	4.06571429	1.88	40698
	2400	0.93566	7.82571429	2	31915
	4800	0.81458	13.5914286	2	41625
	2400	0.83756	12.4971429	1.81	219321
	1200	0.89078	9.96285714	2	47351
	2400	0.8618	11.3428571	2	86957
	4800	0.79334	14.6028571	2	73620
	10000	0.60002	23.8085714	2	56487
	300	0.90578	9.24857143	2	66621
	0	0.96866	6.25428571	0.14	10019

Test SM_03

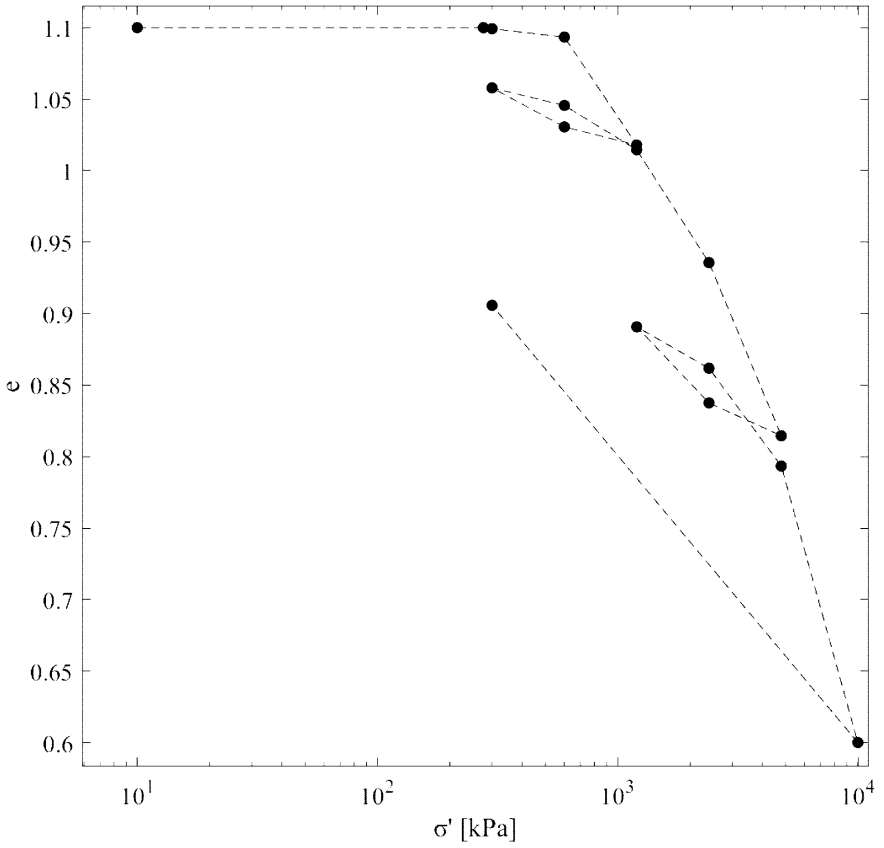

SM_04		e_0	= 1.08	H_0	= 35 mm
	σ' (kPa)	e	eps %	time (weeks)	M (kPa)
	10	1.084	0	-	-
σ' cv	267.12	1.084	0	18.73	-
	300	1.08304731	0.0458022	2	71787
	600	1.07393726	0.48378571	2	68496
	1200	1.03303131	2.45041758	2	30509
	600	1.04035509	2.09831319	2	170404
	300	1.05381177	1.45135714	2	46371
	600	1.04809566	1.72617033	2	109165
	1200	1.02928011	2.63076374	0.17	66328
	2400	0.93442834	7.19094505	2	26315
	4800	0.82695349	12.3580055	2	46448
	2400	0.84779349	11.3560824	1.81	239539
	1200	0.89346286	9.16043956	2	54654
	2400	0.86678766	10.4429011	2	93570
	4800	0.80915017	13.2139341	2	86610
	10000	0.62581771	22.0279945	2	58997
	300	0.90953943	8.38752747	2	71112
	0	0.97301211	5.33595604	0.14	9831

Test SM_04

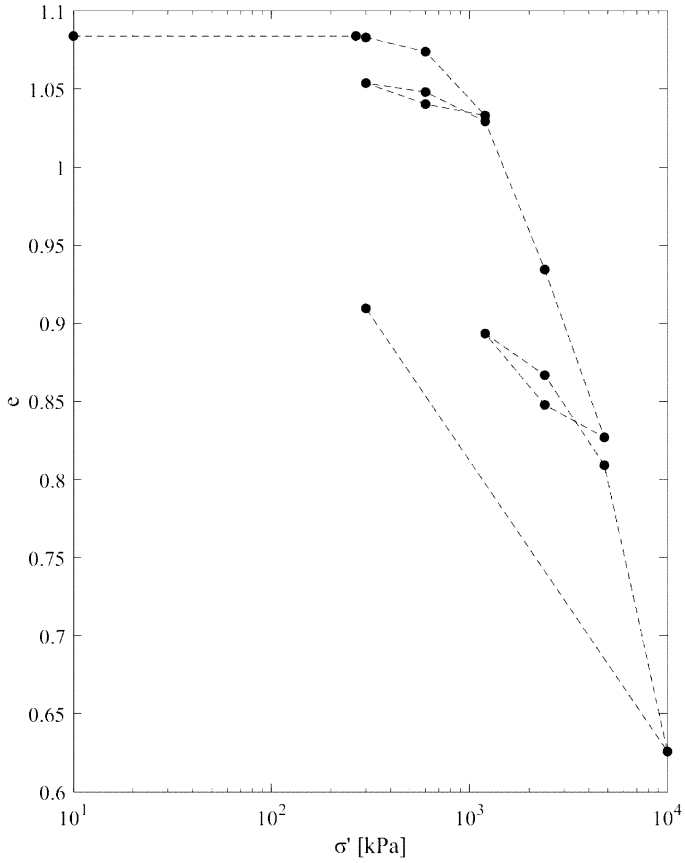

Clays from Nørre Lyngby

Test NL02			e_0 =	0.9	H_0 =	30 mm
Time (day)	**σ' (kPa)**	**ε %**	**e**	**M (kPa)**	**c_v (m^2/s)**	**k (m/s)**
0.06	37.12	0.08	0.90	34696	1.80E-06	5.08E-10
0.71	71.82	0.12	0.90	86739	1.30E-06	1.47E-10
2.18	141.21	0.88	0.88	10130	5.00E-08	4.84E-11
2.84	210.6	1.63	0.87	9190	3.70E-08	3.95E-11
2.98	279.99	2.28	0.86	11192	3.70E-08	3.24E-11
4.00	349.39	2.88	0.85	12391	3.30E-08	2.61E-11
3.10	418.78	3.38	0.84	13474	3.30E-08	2.40E-11
4.11	522.87	4.21	0.82	13786	3.10E-08	2.20E-11
2.81	696.34	5.51	0.80	14827	4.00E-08	2.64E-11
4.06	869.82	6.78	0.77	14457	2.80E-08	1.90E-11
3.18	1043.3	7.85	0.75	21684	5.60E-08	2.53E-11
3.75	1390.26	10.07	0.71	16924	3.70E-08	2.14E-11
4.05	1737.22	11.73	0.68	21286	4.00E-08	1.84E-11
3.32	2084.18	12.95	0.65	27106	6.30E-08	2.28E-11
3.64	2778.09	15.23	0.61	30978	3.70E-08	1.17E-11
4.07	3472.01	16.85	0.58	39995	3.70E-08	9.07E-12
2.01	4512.88	18.58	0.55	55219	3.80E-08	6.74E-12
1.27	5553.75	19.86	0.52	76535	5.60E-08	7.17E-12
2.72	3472.01	19.77	0.52			
0.98	696.34	18.08	0.56			
0.98	71.82	15.89	0.60			
6.00	2.43	11.66	0.68			

Test NL N02

e_0 =	0.90			
e_{fin} =	0.52			
k =	7.17E-12	m/s =	6.20E-07	m/day
k_0 =	5.08E-10	m/s =	4.39E-05	m/day
c_k =	0.203073			
k_x =	1.10E-04	m/day		

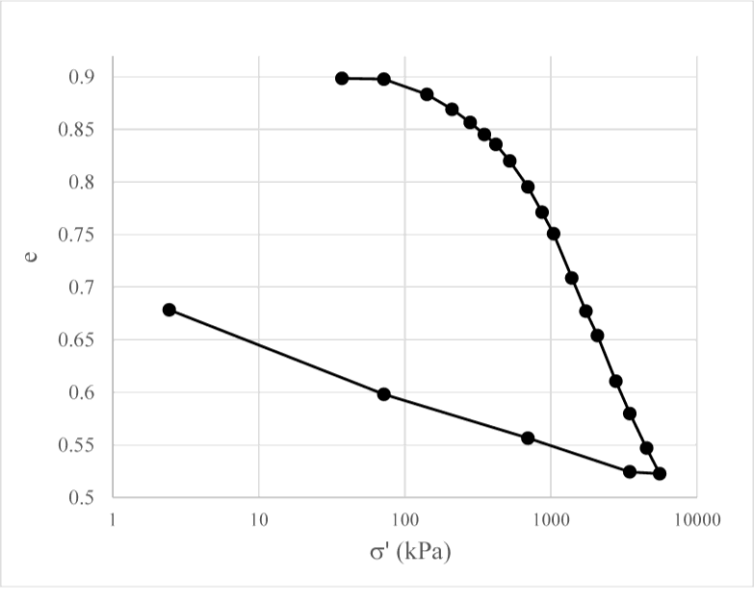

Test NL61			e_0	=1.03	H_0	=30 mm
Time (day)	**σ' (kPa)**	**ε %**	**e**	**M (kPa)**	**c_v (m^2/s)**	**k (m/s)**
0.23	11.1	-0.04	1.03	86739	1.80E-06	2.03E-10
1.70	19.78	-0.05	1.03	-19275	6.70E-08	-3.41E-11
2.92	37.12	0.21	1.03	8068	1.90E-08	2.31E-11
3.19	71.82	1.23	1.01	3988	1.20E-08	2.95E-11
4.84	141.21	2.89	0.97	3876	1.40E-08	3.54E-11
7.20	314.69	4.84	0.93	9082	3.30E-08	3.56E-11
3.85	661.65	7.16	0.88	15420	4.50E-08	2.86E-11
1.91	1008.61	9.23	0.84	20901	5.00E-08	2.34E-11
2.08	1355.56	11.31	0.80	18070	4.50E-08	2.71E-11
2.91	1702.52	13.17	0.76	19713	4.50E-08	2.24E-11
3.00	2396.44	15.92	0.71	26792	4.50E-08	1.65E-11
4.21	3437.31	19.09	0.64	33794	4.00E-08	1.30E-11
24.02	4478.18	21.4	0.60	49098	4.50E-08	7.98E-12
4.06	3437.31	21.27	0.60			
3.70	1355.56	19.83	0.63			
3.04	314.69	16.1	0.70			
2.98	2.43	10.63	0.81			

Tst NL K61

e_0 =	1.03			
e_{fin} =	0.60			
k =	7.98E-12	m/s =	6.90E-07	m/day
k_0 =	2.03E-10	m/s =	1.76E-05	m/day
c_k =	0.31			
k_x =	4.39E-05	m/day		

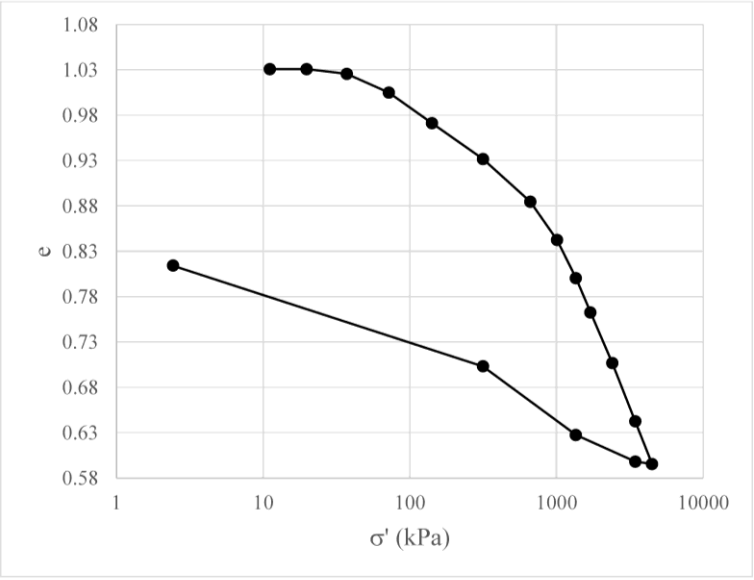

TestNL R02			e_0	= 0.61	H_0	= 30 mm
Time (day)	**σ' (kPa)**	**ε %**	**e**	**M (kPa)**	**c_v (m^2/s)**	**k (m/s)**
	2.4		**0.61**			
0.92	11.1	0.10	0.61	8560	1.60E-05	1.83E-08
1.97	19.8	0.23	0.61	7033	7.20E-06	1.00E-08
4.05	37.1	0.59	0.60	4731	1.60E-05	3.31E-08
1.96	71.8	1.14	0.59	6347	1.60E-05	2.47E-08
1.31	141.2	1.91	0.58	8973	1.60E-05	1.75E-08
2.73	314.7	3.38	0.56	11815	1.60E-05	1.33E-08
2.06	661.6	5.33	0.52	17762	1.60E-05	8.83E-09
1.90	1355.6	7.64	0.49	30148	1.60E-05	5.20E-09
3.04	2743.4	10.12	0.45	55774	1.60E-05	2.81E-09
2.08	4131.2	11.48	0.43	102423	1.60E-05	1.53E-09
1.88	5519.1	12.47	0.41	140421	1.60E-05	1.12E-09
3.00	4131.2	12.42	0.41	3084069	6.50E-05	2.07E-10
2.00	661.6	11.67	0.42	460563	2.50E-05	5.32E-10
2.09	314.7	11.24	0.43	81002	1.60E-05	1.94E-09
4.15	2.4	7.73	0.49	8888	4.00E-06	4.41E-09

Test NL R02

e_0 =	0.61			
e_{fin} =	0.41			
k =	1.12E-09	m/s =	9.65E-05	m/day
k_0 =	1.83E-08	m/s =	1.58E-03	m/day
c_k =	0.16			
k_x =	4.58E-08	m/s =	3.96E-03	m/day

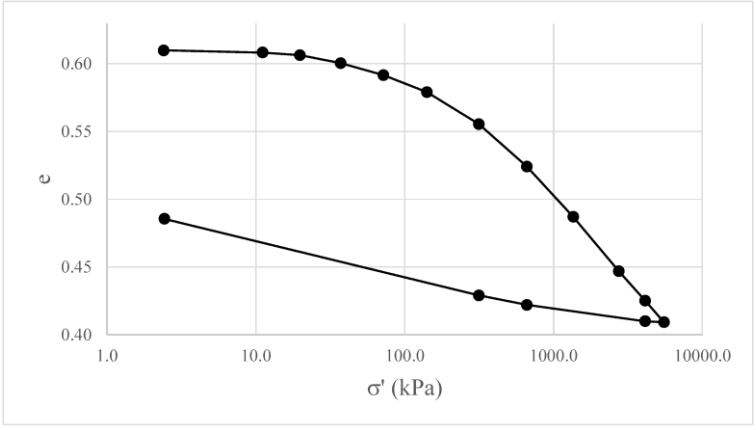

Test NL R01			e_0=	0.78	H0=	30 mm
Time (day)	**σ' (kPa)**	**ε %**	**e**	**M (kPa)**	**c_v (m^2/s)**	**k (m/s)**
0.01	2.4	0	0.78			
2.06	11.1	0.12	0.77	7168	1.80E-07	2.46E-10
3.71	19.78	0.4	0.77	3629	4.00E-08	1.08E-10
1.99	37.12	1.09	0.76	2843	5.00E-08	1.72E-10
1.99	71.82	2.2	0.74	3043	4.30E-08	1.38E-10
3.01	141.21	3.55	0.71	5178	4.50E-08	8.52E-11
1.98	314.69	5.47	0.68	3203	5.60E-08	1.71E-10
2.00	661.65	7.8	0.64	15052	6.30E-08	4.1E-11
4.02	1355.56	10.85	0.58	23602	7.20E-08	2.99E-11
2.99	2743.4	14.23	0.52	42967	8.20E-08	1.87E-11
3.01	4131.23	16.28	0.49	68030	8.20E-08	1.18E-11
2.37	5519.06	17.66	0.46	94410	7.20E-08	7.47E-12
2.05	2743.4	17.37	0.47			
3.57	37.12	12.24	0.56			
13.21	2.43	9.37	0.61			

Test NL R01

e_0 =	0.78			
e_{fin} =	0.46			
k =	7.47E-12	m/s =	6.46E-07	m/day
k_0 =	2.46E-10	m/s =	2.13E-05	m/day
c_k =	0.21			
k_x =	6.15E-10	m/s =	5.32E-05	m/day

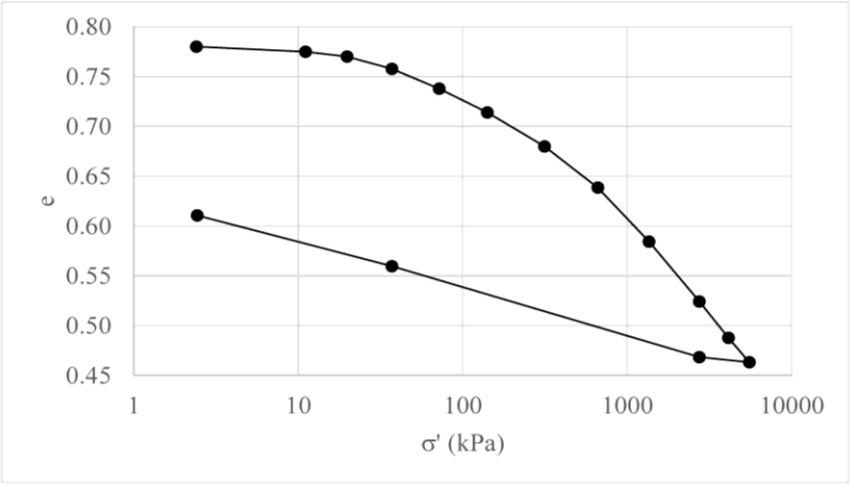

Test NLK10		e_0 =	1.1	H_0 =	30 mm	
Time (day)	**σ' (kPa)**	**ε %**	**e**	**M (kPa)**	**c_v (m^2/s)**	**k (m/s)**
0.20	11.1	0.07	1.10	8674	5.00E-06	5.65E-09
5.73	19.78	0.24	1.09	12391	4.50E-08	3.56E-11
1.98	37.12	1.04	1.08	2090	2.10E-08	9.85E-11
6.00	71.82	2.7	1.04	2168	2.40E-08	1.08E-10
4.30	141.21	4.41	1.01	4130	3.30E-08	7.83E-11
2.72	314.69	7.33	0.95	6151	7.20E-08	1.15E-10
5.03	661.65	13.89	0.81	5542	5.00E-08	8.84E-11
2.19	1008.61	17.61	0.73	10514	4.50E-08	4.19E-11
3.86	1355.56	20.38	0.67	12303	3.30E-08	2.63E-11
2.92	2049.48	24.32	0.59	17049	4.00E-08	2.30E-11
4.01	3090.35	28.16	0.51	27035	5.30E-08	1.92E-11
1.96	4131.23	30.02	0.47	49565	6.30E-08	1.25E-11
2.27	5172.1	31.58	0.44	65054	4.70E-08	7.08E-12
2.81	4131.23	31.55	0.44			
1.21	2049.48	31.32	0.44			
1.75	661.65	30.48	0.46			
3.83	2.43	27.21	0.53			

Test NLK10

e_0 =	1.10			
e_{fin} =	0.44			
k =	7.08E-12	m/s =	6.12E-07	m/day
k_0 =	5.65E-09	m/s =	4.88E-04	m/day
c_k =	0.23			
k_x =	1.41E-08	m/s =	1.22E-03	m/day

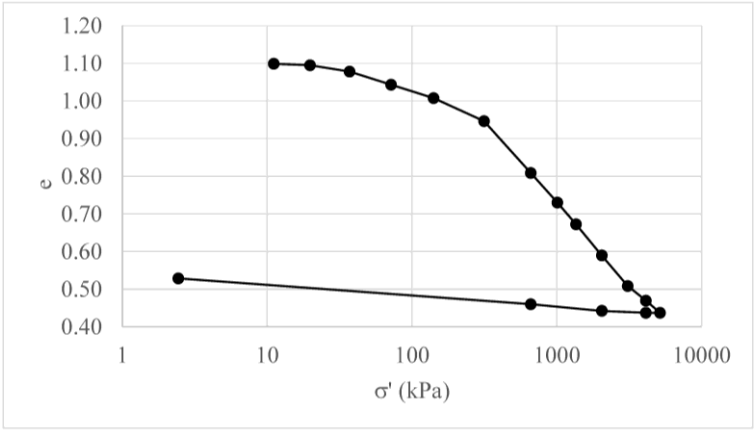

Test NL K16			e_0 =	0.51	H_0 =	30 mm
Time (day)	**σ' (kPa)**	**ε %**	**e**	**M (kPa)**	**c_v (m^2/s)**	**k (m/s)**
	2		0.51			
0.01	11	0.01	0.51	66723	8.20E-06	1.20E-09
0.92	20	0.05	0.51	25512	1.80E-06	6.91E-10
0.86	37	0.10	0.51	40344	4.50E-07	1.09E-10
4.01	72	0.46	0.50	10842	2.50E-07	2.26E-10
3.10	141	1.22	0.49	9377	1.60E-07	1.67E-10
4.08	280	2.33	0.47	12732	3.30E-07	2.54E-10
2.01	627	3.90	0.45	22677	6.50E-07	2.81E-10
2.17	1321	5.65	0.42	40110	1.00E-07	2.44E-11
2.76	3403	8.32	0.38	84623	1.60E-07	1.85E-11
3.87	5137	9.61	0.36	143371	1.30E-07	8.89E-12
3.03	3403	9.57	0.37			
1.08	627	8.73	0.38			
7.91	2	5.67	0.42			

Test NL K16

e_0 =	0.51			
e_{fin} =	0.36			
k =	8.89E-12	m/s =	7.68E-07	m/day
k_0 =	1.20E-09	m/s =	1.04E-04	m/day
c_k =	0.068			
k_x =	3.01E-09	m/s =	2.60E-04	m/day

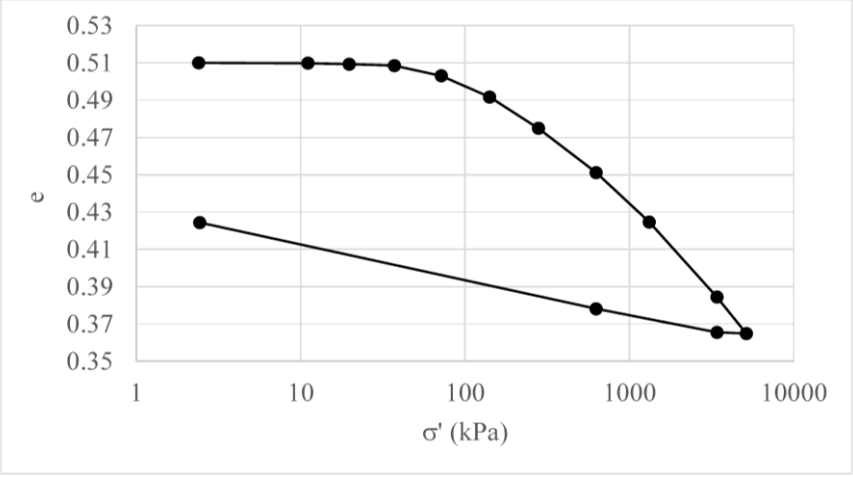

Clays from Anholt

Test A01			e_0 =	0.61	H_0 =	35 mm
Time (day)	**σ' (kPa)**	**ε %**	**e**	**M (kPa)**	**c_v (m^2/s)**	**k (m/s)**
	2.3		0.61			
0.01	8.7	0.00	0.61			
0.04	15.0	-0.02	0.61			
0.05	27.8	0.00	0.61	49020	3.30E-06	6.60E-10
0.04	53.3	0.11	0.61	31086	1.60E-06	5.04E-10
0.72	104.3	0.23	0.61	21974	8.80E-07	3.92E-10
3.00	231.7	0.77	0.60	32266	2.70E-07	8.20E-11
0.98	486.6	1.81	0.58	24557	1.50E-07	5.99E-11
2.00	741.5	2.66	0.57	31200	1.80E-07	5.65E-11
2.15	996.4	3.28	0.56	41516	6.80E-08	1.61E-11
1.85	1251.3	3.80	0.55	46944	4.50E-08	9.39E-12
9.99	1506.2	4.39	0.54	53892	4.50E-08	8.18E-12
4.00	1761.2	4.76	0.53	62172	3.50E-08	5.52E-12
2.00	2525.9	6.03	0.51	64862	1.10E-07	5.29E-12
2.07	4055.3	8.31	0.48	78473	8.60E-08	1.37E-11
0.01	2.3	7.24	0.49			

Test A01

e_0 =	0.61			
e_{fin} =	0.48			
k =	1.37E-11	m/s =	1.19E-06	m/day
k_0 =	6.60E-10	m/s =	5.70E-05	m/day
c_k =	0.08			
k_x =	1.65E-09	m/s =	0.000143	m/day

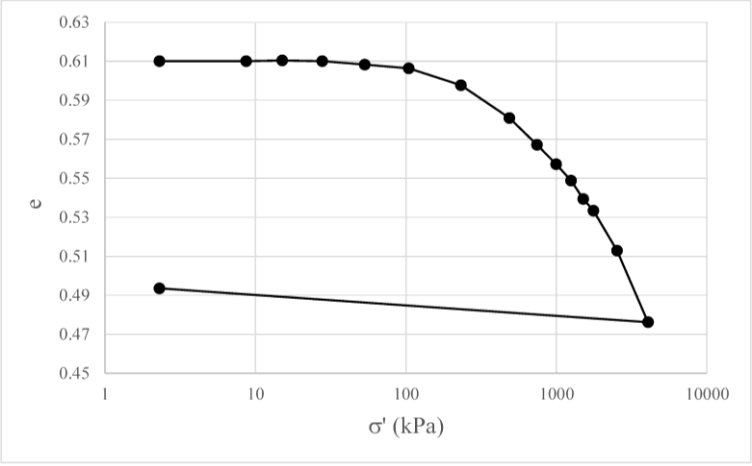

Test A02			e_0 =	0.68	H_0 =	30 mm
Time (day)	**σ' (kPa)**	**ε %**	**e**	**M (kPa)**	**c_v (m^2/s)**	**k (m/s)**
0.01	11.1	-0.01	0.68			
0.04	19.8	-0.10	0.68			
0.04	37.1	-0.10	0.68			
0.04	71.8	-0.08	0.68			
0.69	141.2	-0.01	0.68	49565	1.30E-06	2.57E-10
3.00	314.7	0.39	0.67	59820	6.50E-07	1.06E-10
0.99	661.6	1.38	0.66	35046	2.50E-07	6.99E-11
1.99	1008.6	2.23	0.64	42834	1.60E-07	3.66E-11
2.15	1355.6	2.89	0.63	53378	8.20E-08	1.51E-11
1.84	1702.5	3.45	0.62	60869	5.60E-08	9.02E-12
9.99	2049.5	4.11	0.61	64851	3.30E-08	4.99E-12
4.00	2396.4	4.54	0.60	71982	3.10E-08	4.22E-12
1.99	3437.3	6.07	0.58	74454	7.20E-08	9.48E-12
0.98	5519.1	8.68	0.53	87726	8.20E-08	9.16E-12
0.01	2.4	7.80	0.55			

Test A02

e_0 =	0.68			
e_{fin} =	0.53			
k =	9.16E-12	m/s =	7.91E-07	m/day
k_0 =	2.57E-10	m/s =	2.22E-05	m/day
c_k =	0.101			
k_x =	6.43E-10	m/s =	5.55E-05	m/day

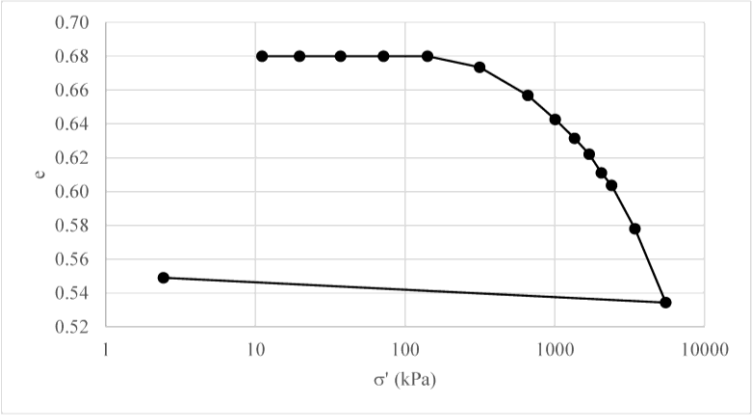

Clays from Skagen

Test S 521			e_0 =	0.67	H_0 =	30 mm
Time (day)	**σ' (kPa)**	**ε %**	**e**	**M (kPa)**	**c_v (m^2/s)**	**k (m/s)**
	2		0.67			
2.87	37	0.83	0.66	4209	4.04E-06	9.41E-09
1.97	72	1.37	0.65	6425	4.04E-06	6.16E-09
2.04	245	2.93	0.62	11109	1.62E-05	1.43E-08
3.02	419	3.83	0.61	19311	4.04E-06	2.05E-09
1.98	592	4.47	0.60	27036	4.04E-06	1.46E-09
1.97	939	5.48	0.58	34239	7.18E-06	2.06E-09
3.03	1286	6.25	0.57	45354	1.79E-06	3.87E-10
2.05	1980	7.34	0.55	63468	7.18E-06	1.11E-09
1.93	3021	8.58	0.53	83941	1.62E-05	1.89E-09
3.04	4409	9.86	0.51	108283	7.18E-06	6.50E-10
1.95	6144	11.04	0.49	147432	7.18E-06	4.77E-10
28.04	5450	11.06	0.49	-2602183	1.62E-05	-6.10E-11
5.09	6144	11.24	0.48	392782	1.62E-05	4.04E-10
1.98	5450	11.23	0.48	4626104	1.62E-05	3.43E-11
1.91	1980	10.98	0.49	1406586	6.47E-05	4.51E-10
1.43	72	10.16	0.50	231773	6.47E-05	2.74E-09
7.33	2	9.35	0.51	8620	1.62E-07	1.84E-10

Test S521

e_0 =	0.66			
e_{fin} =	0.49			
k =	4.77E-10	m/s =	4.12E-05	m/day
k_0 =	9.41E-09	m/s =	8.13E-04	m/day
c_k =	0.13			
k_x =	2.35E-08	m/s =	2.03E-03	m/day

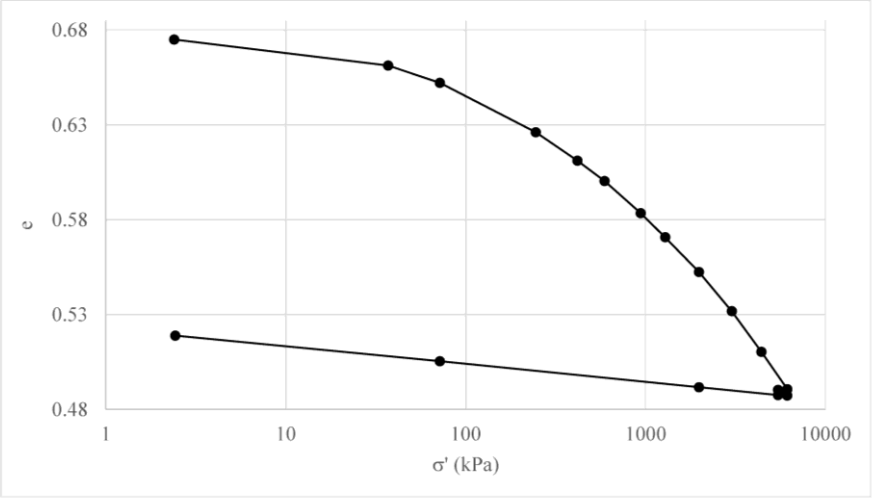

Test S524			e_0 =	0.75	H_0 =	30 mm
Time (day)	**σ' (kPa)**	**ε %**	**e**	**M (kPa)**	**c_v (m^2/s)**	**k (m/s)**
	2		**0.75**			
1.88	37	0.55	0.74	6425.1	1.62E-05	2.47E-08
3.00	72	0.91	0.73	10204	7.18E-06	6.90E-09
2.00	245	2.08	0.71	15770.8	1.62E-05	1.01E-08
2.09	419	3.04	0.70	19492	7.18E-06	3.61E-09
2.94	766	4.91	0.66	24961	7.18E-06	2.82E-09
2.23	1460	7.21	0.62	29654.5	1.12E-05	3.70E-09
1.74	2154	8.63	0.60	44768.7	7.18E-06	1.57E-09
3.00	3194	10.28	0.57	65463.7	7.18E-06	1.07E-09
3.04	4582	11.91	0.54	88963.5	7.18E-06	7.91E-10
2.00	5970	13.06	0.52	106756.2	7.18E-06	6.59E-10
2.08	7358	14.00	0.50	150851.2	7.18E-06	4.66E-10
1.96	5970	13.97	0.51			
5.02	766	13.42	0.52			
1.89	245	13.11	0.52			
5.00	2	11.23	0.55			

Test S524

e_0 =	0.74			
e_{fin} =	0.50			
k =	4.66E-10	m/s =	4.03E-05	m/day
k_0 =	2.47E-08	m/s =	2.13E-03	m/day
c_k =	0.14			
k_x =	6.18E-08	m/s =	5.34E-03	m/day

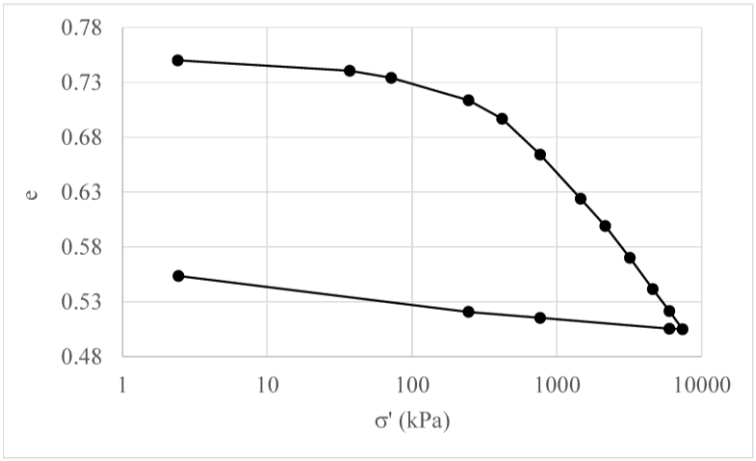

Aalborg Clay

Test Y_01

	e_0 =	0.97	H_0 =	35 mm
Time (day)	**σ' (kPa)**	**e**	**ε %**	**M (kPa)**
2.76	38	0.97	0	-
3	76	0.96	0.68	5599.438
2	153	0.92	2.36	4555.798
2	76	0.93	1.95	18587.02
2.83	153	0.92	2.49	14124.18
2	306	0.87	4.92	6297.721
2	612	0.80	8.40	8793.532
2.83	1224	0.72	12.49	14947.47
2.17	2498	0.64	16.83	29405.97
4.53	1224	0.65	16.40	296404.4
2	612	0.67	15.32	57023.31
1.83	1224	0.66	15.75	143706.4
4	2498	0.63	17.23	86034.44
5.83	5047	0.55	21.36	61721.01
9.83	0	0.88	4.50	

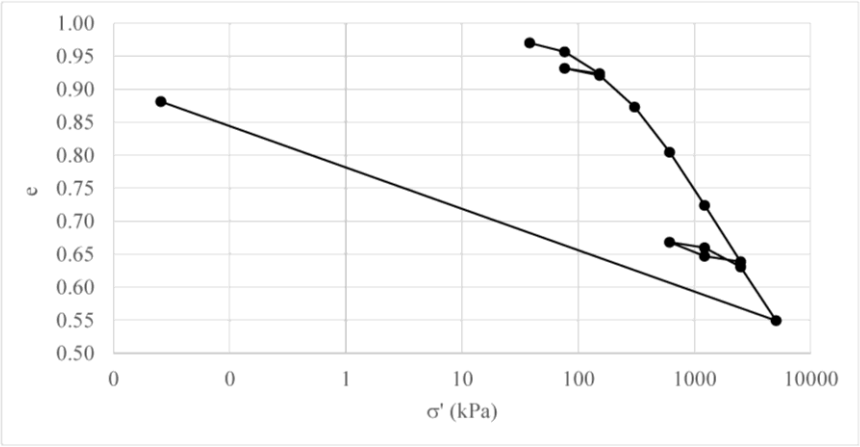

Test Y_02

	e_0 =	0.88	H_0 =	35 mm
Time (day)	**σ' (kPa)**	**e**	**ε %**	**M (kPa)**
2.58	38.24	0.88	0	
3	76.47	0.87	0.30	12868
2	152.94	0.85	1.62	5775
2	76.47	0.85	1.37	30073
2.83	152.94	0.85	1.68	24113
2	305.89	0.81	3.72	7518
2	611.78	0.75	6.90	9602
2.83	1223.56	0.67	10.87	15438
2.17	2498.10	0.59	15.30	28734
4.53	1223.56	0.60	14.71	216024
2	611.78	0.62	13.73	62336
1.83	1223.56	0.61	14.27	112993
4	2498.10	0.58	15.80	83459
5.83	5047.17	0.50	20.05	59918
10	0.03	0.75	6.72	

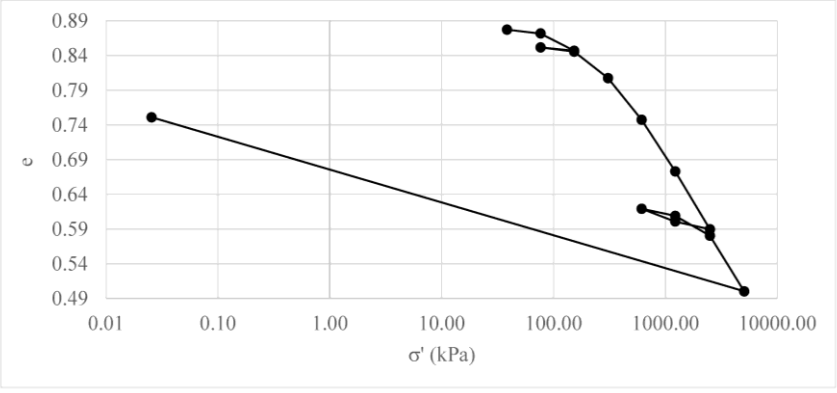

Test Y_03

	e_0 =	0.86	H_0 =	35 mm
Time (day)	**σ' (kPa)**	**e**	**ε %**	**M (kPa)**
2.60	38	0.86	0	
3	76	0.85	0.18	21075
2	153	0.85	0.72	14313
2	76	0.85	0.65	111522
2.83	153	0.84	0.76	69520
2	306	0.82	2.23	10404
2	612	0.77	4.78	11969
2.83	1224	0.71	8.06	18684
2.17	2498	0.63	12.04	32012
4.52	1224	0.64	11.92	1037415
2	612	0.64	11.49	142274
1.83	1224	0.64	11.51	3058893
3.17	2498	0.63	12.42	139621
5.83	5047	0.55	16.55	61742
10	0	0.79	3.48	38621

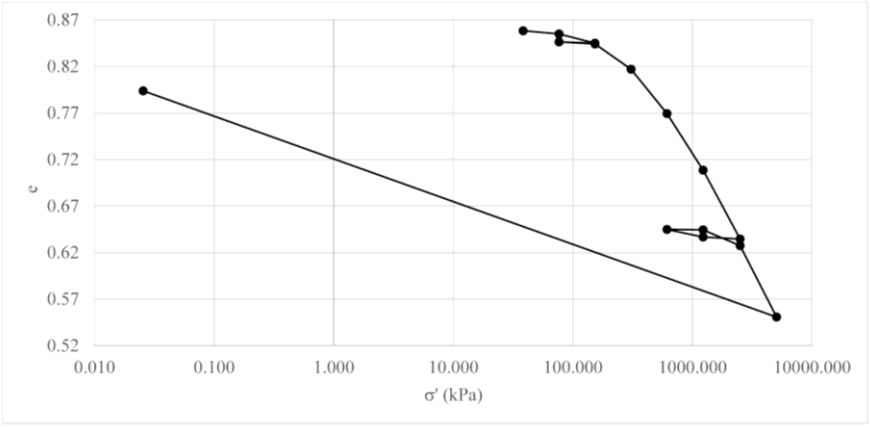

Test Y_04

	e_0 =	0.84	H_0 =	35
Time (day)	**σ' (kPa)**	**e**	**ε %**	**M (kPa)**
2.60	38.24	0.84	0	
3	76.47	0.83	0.45	8476
2	152.94	0.82	1.47	7519
2	76.47	0.82	1.20	28524
2.83	152.94	0.82	1.52	23960
2	305.89	0.79	3.08	9793
2	611.78	0.74	5.60	12121
2.83	1223.56	0.68	8.83	18949
2.17	2498.10	0.61	12.67	33204
4.50	1223.56	0.62	12.26	306657
2	611.78	0.63	11.37	69116
1.83	1223.56	0.62	11.77	155138
4	2498.10	0.60	13.06	98628
5.83	5047.17	0.53	16.71	69706
10	0.03	0.78	3.39	37888

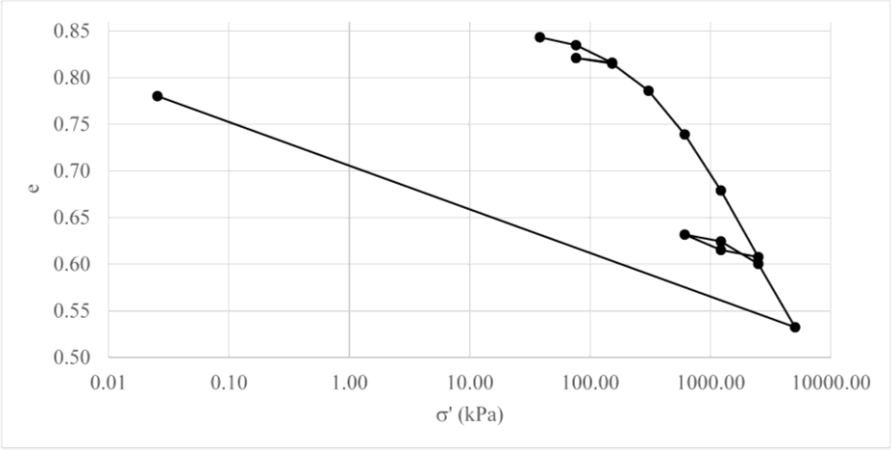

Clays from Rømø

Test R01	e_0	= 0.82	H_0	= 20 mm
Time (day)	**σ' (kPa)**	**ε %**	**e**	**M (kPa)**
	5	0	0.82	-
0.01	103	0.42	0.81	23212
0.18	202	0.78	0.81	27945
1.68	398	1.98	0.78	16245
1.01	790	3.75	0.75	22198
3.02	1477	5.94	0.71	31340
0.99	2948	8.72	0.66	53038
0.98	5891	12.31	0.60	81919
6.04	11777	17.40	0.50	115591
2.83	20606	21.61	0.43	209843

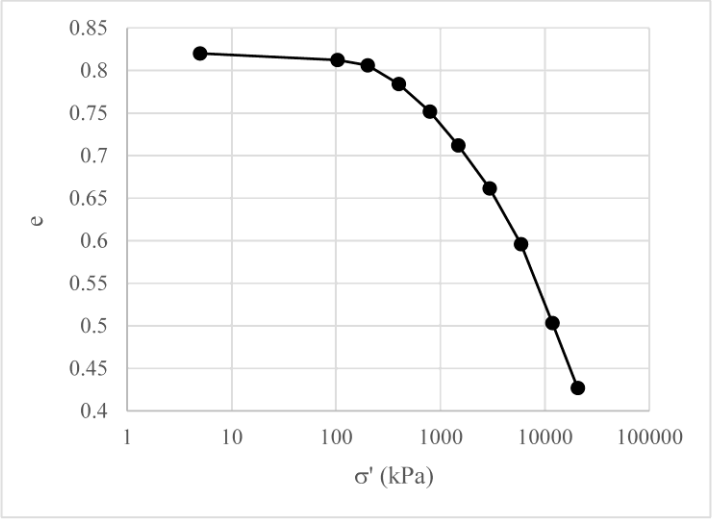

Test R341	e_0	= 0.68	H_0	= 30 mm
Time (day)	**σ' (kPa)**	**ε %**	**e**	**M (kPa)**
	2	0.00	0.68	-
0.08	176	0.72	0.67	24210
0.85	349	1.68	0.65	18039
1.00	696	3.37	0.62	20510
1.10	1390	5.44	0.59	33577
3.02	2431	7.48	0.55	50898
2.00	3819	9.30	0.52	76535
2.01	5207	10.72	0.50	97506
2.95	6595	11.94	0.48	113447
3.96	7982	12.96	0.46	136508
3.04	8676	13.36	0.46	171337

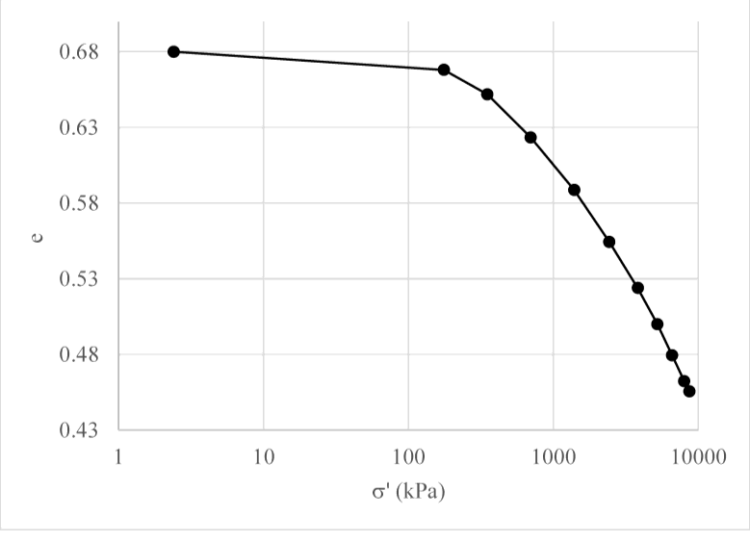

Test ¤R343	e_0 = 0.73		H_0 = 30 mm	
Time (day)	**σ' (kPa)**	**ε %**	**e**	**M (kPa)**
	2	0	0.73	-
1.74	176	0.60	0.72	28758
4.21	349	2.17	0.69	11050
3.03	696	4.77	0.65	13387
3.77	1390	8.18	0.59	20320
3.03	2431	11.07	0.54	36037
4.05	3819	13.78	0.49	51275
3.90	5207	15.54	0.46	78556
4.00	6595	16.86	0.44	105139
3.27	7982	17.89	0.42	134959
6.87	8676	18.61	0.41	95933

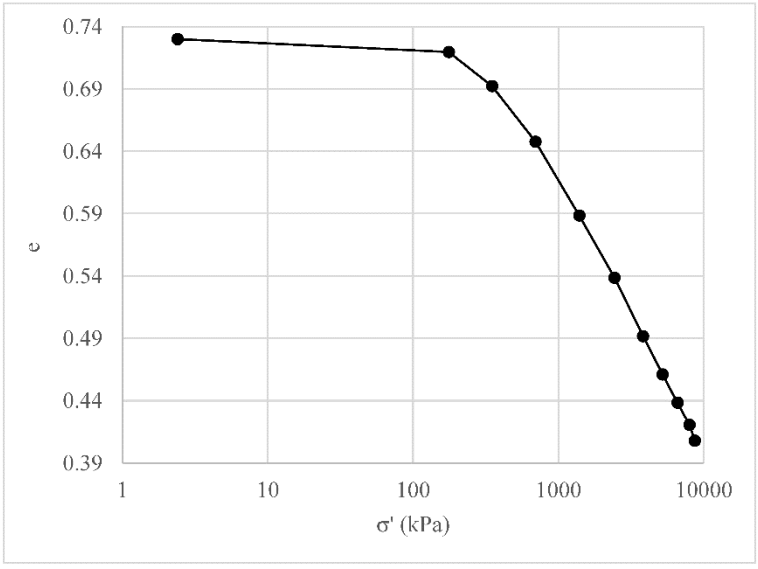

ISSN (online): 2446-1636
ISBN (online): 978-87-7210-893-3 AALBORG UNIVERSITY PRESS